Numerical studies in rotating and stratified turbulence

by

Enrico Deusebio

December 2013
Technical Report
Royal Institute of Technology
Department of Mechanics
SE-100 44 Stockholm, Sweden

Akademisk avhandling som med tillstånd av Kungliga Tekniska Högskolan i Stockholm framlägges till offentlig granskning för avläggande av teknologie doktorsexamen fredagen den 17 januari 2014 kl10.00i Kollegiesalen, Kungliga Tekniska Högskolan, Brinellvägen 8, Stockholm.

©Enrico Deusebio 2013 Tryckt av Eprint AB 2013

Numeriska simuleringar av roterande och stratifierad turbulens

Enrico Deusebio

Linné Flow Centre, KTH Mechanics, Royal Institute of Technology SE-100 44 Stockholm, Sweden

Sammanfattning

En grundlig vetenskaplig förståelse av turbulens saknas fortfarande, fastän fenomenet har studerats i fem hundra år. Vid sidan av observationer och experiment kan beräkningar med hjälp av kraftfulla datorer idag ge oss en del insikter i turbulensens dynamik. I denna avhandling presenteras simuleringar av såväl homogen turbulens som turbulens i strömningar i närvaro av en vägg. I båda fallen studeras en roterande och stratifierad fluid, så som är fallet i geofysikaliska strömningar där jordrotationen och den vertikala densitetsvariationen har stort inflytande.

För homogen turbulens undersöker vi hur energiutbytet mellan olika turbulenta skalor påverkas av stark men ändlig rotation och stratifiering. Till skillnad från kvasigeostrofisk turbulens, visar vi att det existerar en energikaskad mot mindre skalor som initieras vid den skala vid vilken turbulensen exciteras. Vid stora skalor är denna process av underordnad betydelse, men vid mindre skalor kommer den att dominera. Vid dessa skalor ser man därför att vågtalsspektrum av den turbulenta energin genomgår en övergång från k^{-3} till $k^{-5/3}$. Tvåpunktsstatistik visar en god överenstämmelse med mätningar från atmosfären, vilket talar för att energikaskaden mot mindre skalor är en betydelsefull process i atmosfären.

Ett gränsskikt i ett roterande system i vilket rotationsaxeln är normal mot väggen brukar kallas ett Ekmanskikt, vilket kan ses som en modell för de gränsskikt som utvecklar sig i atmosfären och oceanerna. Vi studerar den turbulenta dynamiken i Ekmanskiktet med hjälp av numeriska simuleringar, med speciellt fokus på de strukturer som utvecklas vid måttliga Reynoldstal. För neutralt skiktade fluider visar vi att det finns en turbulent kaskad av helicitet i det logaritmiska skiktet. Vi fokuserar också på effekten av en stabil skiktning som uppstår på grund av en vertikal temperaturgradient. Om skiktningen inte är alltför stark, observerar vi en turbulent dynamik som i stort sett överenstämmer med existerande teorier och modeller som används för atmosfäriska gränsskikt. För starkare skiktning visar vi att det finns samexisterande turbulenta och laminära områden som visar sig i snett löpande band i förhållande till medelhastigheten, i stor likhet med vad som nyligen observerats i andra strömningar som genomgår transition mellan ett laminärt och turbulent tillstånd.

Numerical studies in rotating and stratified turbulence

Enrico Deusebio

Linné Flow Centre, KTH Mechanics, Royal Institute of Technology SE-100 44 Stockholm, Sweden

Abstract

Although turbulence has been studied for more than five hundred years, a thorough understanding of turbulent flows is still missing. Nowadays computing power can offer an alternative tool, besides measurements and experiments, to give some insights into turbulent dynamics. In this thesis, numerical simulations are employed to study homogeneous and wall-bounded turbulence in rotating and stably stratified conditions, as encountered in geophysical flows where the rotation of the Earth as well as the vertical density variation influence the dynamics.

In the context of homogeneous turbulence, we investigate how the transfer of energy among scales is affected by the presence of strong but finite rotation and stratification. Unlike geostrophic turbulence, we show that there is a forward energy cascade towards small scales which is initiated at the forcing scales. The contribution of this process to the general dynamic is secondary at large scales but becomes dominant at smaller scales where it leads to a shallowing of the energy spectrum, from k^{-3} to $k^{-5/3}$. Two-point statistics show a good agreement with measurements in the atmosphere, suggesting that this process is an important mechanism for energy transfer in the atmosphere.

Boundary layers subjected to system rotation around the wall-normal axis are usually referred to as Ekman layers and they can be seen as a model of the atmospheric and oceanic boundary layers developing at mid and high latitudes. We study the turbulent dynamics in Ekman layers by means of numerical simulations, focusing on the turbulent structures developing at moderately high Reynolds numbers. For neutrally stratified conditions, we show that there exists a turbulent helicity cascade in the logarithmic region. We focus on the effect of a stable stratification produced by a vertical positive temperature gradient. For moderate stratification, continuously turbulent regimes are produced which are in fair agreement with existing theories and models used in the context of atmospheric boundary layer dynamics. For larger degree of stratification, we show that laminar and turbulent motions coexist and displace along inclined patterns similar to what has been recently observed in other transitional flows.

Descriptors: Geostrophic turbulence, stable stratification, rotation, wall-bounded turbulence, gravity waves, atmospheric dynamics, direct numerical simulations

Preface

This thesis contains numerical investigations of stratified and rotating turbulence, both with and without the presence of walls. A brief introduction on the basic concepts and methods is presented in the first part. The second part contains six articles and one internal report. The papers are adjusted to comply with the present thesis format for consistency, but their contents have not been altered as compared with their original counterparts.

Paper I. A. Vallgren, E. Deusebio & E. Lindborg, 2011 Possible explanation of the atmospheric kinetic and potential energy spectra. *Phys. Rev. Lett.*, 107:26, 268501.

Paper II. E. DEUSEBIO, A. VALLGREN & E. LINDBORG, 2013 The route to dissipation in strongly stratified and rotating flows. *J. Fluid Mech.*, 720, 66-103, 2013

Paper III. E. DEUSEBIO, A. AUGIER & E. LINDBORG, 2013 Third order structure functions in rotating and stratified turbulence: analytical and numerical results compared with data from the stratosphere. *Submitted to J. Fluid Mech.*

Paper IV. E. DEUSEBIO, G. BOFFETTA, S. MUSACCHIO & E. LINDBORG, 2013

Dimensional transition in rotating turbulence Submitted to Phys. Rev. E

Paper V. E. Deusebio, G. Brethouwer, P. Schlatter & E. Lindborg, 2013

A numerical study of the unstratified and stratified Ekman layer. *Under revision for publication in J. Fluid Mech.*

Paper VI. E. DEUSEBIO & E. LINDBORG, 2013 Helicity in the Ekman boundary layer. Submitted to J. Fluid Mech. Rapids

Paper VII. E. DEUSEBIO, 2012 The open-channel version of SIMSON *Internal Report*

Division of work among authors

The main advisor for the project is Dr. Erik Lindborg (EL). Dr. Philipp Schlatter (PS) and Dr. Geert Brethouwer (GB) have acted as co-advisors.

Paper I

The code was developed and implemented by Andreas Vallgren (AV) and Enrico Deusebio (ED). The numerical simulations were performed by AV. The paper was written by EL, with the help of AV and ED. ED was particularly active during the review process.

Paper II

The solver code was developed and implemented by ED in collaboration with AV. The numerical simulations were performed by ED. The post-processing code for studying the triad interactions was developed by ED. The paper was written by ED, with the help of EL. AV provided comments on the article.

Paper III

The simulations and the post-processing were carried out by ED with input from EL and Pierre Augier (PA). The paper was written by ED, EL and PA.

Paper IV

The code which has been used in the study was provided by Guido Boffetta (GB) and Stefano Musacchio (SM). ED implemented an implicit scheme for adding the contribution of rotation and for I/O operations. ED carried out the simulations with input from GB and SM. The paper was written by GB, SM and ED with feedback from EL.

Paper V

The modification of the existing code SIMSON was performed by ED, with the help of PS and GB. The simulations and the analysis of the results were done by ED, with the input of PS, GB and EL. The paper was written by ED, with feedback by EL, GB and PS.

Paper VI

The post-processing of the data was done by ED with input from EL. The paper was written by ED, with feedback by EL.

Paper VII

The idea underlying the new discretisation was suggested by EL. The implementation, code-optimisation and validation were done by ED, under supervision of PS, GB and EL. The report was written by ED.

Part of the work has also been presented at the following international conferences:

E. Deusebio, A. Vallgren & E. Lindborg

Quasi-geostrophic turbulence at finite Rossby number. 7^{th} International Symposium of Stratified Flows - Rome 2011.

E. Deusebio, P. Schlatter, G. Brethouwer & E. Lindborg Direct numerical simulations of stratified open-channel flows. 13^{th} European Turbulence Conference - Warsaw 2011.

A. Vallgren, E. Deusebio & E. Lindborg

Quasi-geostrophic turbulence at finite Rossby number. 13^{th} European Turbulence Conference - Warsaw 2011.

E. Deusebio & E. Lindborg

The role of geostrophy and ageostrophy in rotating and stratified systems. 9^{th} European Fluid Mechanics Conference - Rome 2012.

E. Deusebio & E. Lindborg

Pathways to dissipation in strongly rotating and stratified turbulent systems. 65^{th} Annual Meeting of the APS Division of Fluid Dynamics - San Diego, 2012.

E. DEUSEBIO, P. SCHLATTER, G. BRETHOUWER & E. LINDBORG Direct numerical investigation of the stably-stratified Ekman layer. 14^{th} European Turbulence Conference - Lyon, 2013.



Perché tu non perda mai la direzione, e perché, se mai la perdessi, questo ti guidi verso le persone che ti vogliono bene (N. Mokbel)

Sammanfattning	iii
Abstract	iv
Preface	V
Part I - Introduction	1
Chapter 1. Turbulence and numerical simulations	3
Chapter 2. Rotating and stratified turbulence: a geophysical perspective	8
2.1. Geostrophic turbulence	9
2.2. Stratified turbulence	12
2.3. Three-dimensional turbulence	13
2.4. Rotating turbulence	14
2.5. Towards the atmosphere	17
Chapter 3. Stratified and rotating turbulence in the presence of	
walls	22
3.1. The scales of motions in wall-bounded turbulence	22
3.2. Numerical grids in wall-bounded flows	26
3.3. Rotating wall-bounded flows	27
3.4. Stratified wall-bounded flows	31
Chapter 4. Summary of the papers	37
4.1. Homogeneous turbulence close to geostrophic conditions	37
4.2. Wall bounded stratified turbulence	38
Chapter 5. Conclusions and outlook	41
5.1. Turbulence close to geostrophy: A key for improving weather forecast	41
5.2. Wall-bounded turbulence and atmospheric boundary layers	43
·	
Acknowledgments	45
Bibliography	47
Part II - Papers	57
Possible explanation of the atmospheric kinetic and potential energy spectra	61
The route to dissipation in strongly stratified and rotating flows	s 73

Third order structure function in rotating and stratified turbulence: analytical and numerical results compared with data				
from the stratosphere	119			
Dimensional transition in rotating turbulence	141			
A numerical study of the unstratified and stratified Ekman layer	157			
Helicity in the Ekman boundary layer	199			
The open-channel version of SIMSON	213			

Part I Introduction

CHAPTER 1

Turbulence and numerical simulations

"Observe the motion of the surface of the water which resembles that of hair, and has two motions, of which one goes on with the flow of the surface, the other forms the lines of the eddies; thus the water forms eddying whirlpools one part of which are due to the impetus of the principal current and the other to the incidental motion and return flow¹." It was between the XV and the XVI century that the first attempt of a scientific study of turbulent motions was done by the Italian Leonardo da Vinci. More than five hundred years later, turbulence is still not fully understood and many of its aspects remain mysterious. Richard Feynman describes turbulence as one of the most important unsolved problem of classical physics (Feynman 1964). The note left by Leonardo da Vinci already contains a description of some important characteristic features of turbulence: the presence of eddies and swirling motions which, in a rather chaotic manner, superimpose on the main motion of the fluid. It was the same observation which led Reynolds (1895), almost four hundred years later, to describe turbulent motions statistically by decomposing the velocity field into a mean and a fluctuating part. Indeed, the perhaps most important insight into the essentials of turbulence goes back to less than a hundred years ago, with the observations of Richardson (1922)

> Big whirls have little whirls that feed on their velocity, and little whirls have lesser whirls and so on to viscosity

Far from being trivial, Richardson's observation constitutes the ground on which all the following theories were based (e.g. Kolmogorov 1941a). Large eddies break down into smaller eddies in an inviscid process which continues until kinetic energy is converted into heat at the very smallest scales of motions where viscosity dominates. Thus, turbulent flows possess many scales, both in space and in time, and they own their intrinsic complexity to the interplay among these scales.

From a historical perspective, most of the advances in the understanding of turbulent processes were made in the past hundred years, since the pioneer work of Reynolds (1886). Besides the experimental investigations, a substantial

 $^{^{1}\}mathrm{see}$ Richter, J. P. 1970. Plate 20 and Note 389. In The Notebooks of Leonardo Da Vinci. New York: Dover Publications.

1. TURBULENCE AND NUMERICAL SIMULATIONS



FIGURE 1.1. da Vinci sketch of a turbulent flow

amount of work has also been dedicated to theoretical investigations of turbulence. Several approaches were proposed and undertaken. Strongly influenced by the view of turbulent motions as chaotic and unpredictable, the early studies mainly aimed at a statistical characterization of the dynamics.

Perhaps the most important contribution to a quantitative statistical description of turbulent flows is the theory proposed by Kolmogorov (1941a). As eddies break down into smaller eddies, they lose any preferable orientation and the anisotropy of the large scales of the flow is progressively lost. Kolmogorov (1941a) suggested that statistical quantities in the cascade neither depend on the direction nor on the spatial coordinates, but they attain an universal form which depends only on the energy flux through the cascade, ε , and, at small scales, on the viscosity ν . Despite its simplicity, Kolmogorov (1941a) theory has been able to make quantitatively accurate predictions.

The apparent chaotic and unpredictable nature of turbulent flows seems to be in contrast with the deterministic nature of the Navier-Stokes equations which govern the fluid motions. Besides the *statistical* approach, other approaches have also been proposed, postulating the presence of more organized patterns. The *structural* approach aims at identifying coherent structures which cyclically appears in the flow and sustain the turbulent motions. The *deterministic* approach, on the other hand, views a turbulent process as a nonlinear dynamical system which exhibits a high dependence on initial conditions and apparently chaotic solutions which, however, project onto particular objects in phase-space, called "strange attractors".

In the last fifty years turbulence research has benefited from the powerful tool of digital computers, which complementary to experiments, can be used to study turbulence in detail. This thesis shows how such an approach can be effectively employed in order to shed light on turbulent dynamics. As opposed to experiments, numerical simulations give full information of flow fields and also allow a perfect control of external conditions (e.g. boundary conditions). Moreover, they also allow us to study idealized and "non-physical" setups where different factors/phenomena influencing the turbulent dynamics can be separated.

The first attempt to carry out a direct flow computation was made in the beginning of the XX century by Richardson (1922), who undertook the first historical weather forecast ever done. The measured atmospheric data were advanced in time by using a rather simple mathematical model able to capture the main features of the atmosphere, predicting the flow evolution in the next six hours. All the computations were done by hand. Unfortunately, because some smoothing techniques were not applied on the original data, Richardson's forecast failed dramatically. Nevertheless, it represents a mile-stone in the soon-to-appear era of numerical simulations.

It was only in the beginning of the 1960 that the technology of the digital computers were sufficiently developed to allow for the first numerical computations. Lorenz (1963) studied a simple version of the Navier-Stokes equations in his pioneer work based on machine computations. The system studied by Lorenz (1963) was nonlinear and deterministic, as the Navier-Stokes equations. Moreover, it shared some common features with turbulent motions, such as high sensitivity to initial conditions and chaotic solutions. The work of Lorenz resolved the apparent paradox that deterministic systems can behave chaotically, delineating the beginning of the modern view of turbulence as "deterministic chaos".

From a numerical perspective, the most challenging aspect of turbulence is its intrinsic feature of containing a large range of scales that interact with each other. If one aims at correctly simulating turbulent flows, all the scales, from the large energy-containing scales to the very smallest scales, must be represented, posing severe computational requirements. In the atmosphere, for instance, the largest scales are of the order of thousand kilometres. On the other hand, viscosity acts at millimetre scales. To represent such a vast span of scales in a simulation is, of course, impossible. Also numerical computations of turbulent flows in typical engineering applications, such as flows around aircraft or cars, are still out of reach. The largest scale of turbulence is often referred to as the integral length scale L, whereas the smallest scale is the Kolmogorov scale, defined as $\eta = \nu^{3/4}/\varepsilon^{1/4}$. The Kolmogorov scale is usually interpreted as the scale at which viscosity acts and dissipates the downscale-cascading energy. A fundamental parameter in fluid dynamic applications is the Reynolds number, $Re = UL/\nu$, which quantifies the relative importance between inertial and viscous forces. Here, U is a characteristic large scale velocity. The ratio between the largest scale, L, and the smallest viscosity affected scale, η , can be related to the Reynolds number as $L/\eta \sim Re^{3/4}$. Values of Re are typically of the order of 10^9 in geophysical applications and 10^6 in engineering applications, making the computation of such flows out of reach at the present point.

The first pioneer direct numerical simulations of a homogeneous and isotropic turbulent flow dates back to the beginning of the 70s, with the work of Orszag & Patterson (1972). The scale separation simulated was indeed very limited, with 64^3 grid points, very far from being of practical interest. Early attempts to numerically describe turbulent flows were instead deeply connected with the development of mathematical models of turbulent motions.

The idea of replacing the exact Navier-Stokes equations with its filtered/averaged counterparts goes back to the decomposition of Reynolds (1895). The filtered scale-independent Reynolds Averaged Navier-Stokes (RANS) equations, still exact, contain terms which are not closed and therefore need to be modelled. In other words, a model for the turbulent fluctuations must be constructed. The first attempt to model turbulence was proposed by Boussinesq (1877), who suggested an analogy between turbulent motions and the Brownian motion of gas molecules. He postulated that the effect of turbulent motions in the flow can be modelled by a fictitious eddy-viscosity. Despite its simplicity and its limitations, the general idea of Boussinesq is still widely used in many current turbulent models.

Besides the efforts on improving the models of RANS, new approaches were also proposed in the early 70s, such as Large-Eddy Simulations (LES) (Smagorinsky 1963; Deardorff 1970). The underlying idea of these new approaches was to resolve the turbulent scales to a certain extent and model the remaining part, the so called sub-grid scales. However, as pointed out by Reynolds (1990), before the 90s computational power had not increased enough to make even LES feasible, and only RANS were actually used in engineering applications. However, since LES became feasible, it has been the subject of an increasing amount of studies and represents the perhaps most promising technique of modelling turbulent flows. Recent developments in the field of the LES includes the dynamic procedure proposed by Germano (1992) and Germano et al. (1991), various forms of "synthetic-velocity" (Domaradzki & Saiki 1997), approximate deconvolution models (Stolz & Adams 1999) and explicit algebraic models (Gatski & Speziale 1993; Rasam et al. 2011).

In the 90s, computational resources had reached a maturity which made DNS at reasonably high Reynolds numbers possible. Besides the study of homogeneous isotropic turbulence at high Reynolds numbers, turbulent flows in the presence of solid walls were also investigated. The first DNS of a fully turbulent channel flow was performed by Kim et al. (1987). Interestingly, such a study was shortly preceded by a DNS of the curved channel by Moser & Moin (1987). The turbulent flat-plate boundary layer was first investigated by Spalart (1988). In the following years, a large number of studies were carried out. The complexity of the flows gradually increased by considering compressible, even reacting, flows and several non-trivial geometries. The evolution of

the geometries also led to the development of new numerical methods able to deal with curved and irregular walls.

Nevertheless, as noted by Moin & Mahesh (1998), it was still impossible to simulate flows with Reynolds numbers comparable to experiments. The development of massively parallel machines over the last decade has made it feasible to increase the Reynolds number by almost one order of magnitude. In the field of isotropic and homogeneous turbulence, a DNS at resolution 4096³ was performed by Kaneda et al. (2003). In the field of wall-bounded flows, a simulation of a channel flow at a friction Reynolds number² $Re_{\tau} = 2000$ was performed by Hoyas & Jiménez (2006), whereas its turbulent boundary layer counterparts were studied by Schlatter et al. (2009) at a Re_{θ} , defined with the momentum thickness³ θ in place of L, of $Re_{\theta} = 2500$ and Sillero et al. (2013) at $Re_{\theta} = 6000$. Nowadays, the Reynolds number that can be reached in numerical simulations and in experiments are comparable, allowing for a comparison and a complementary analysis (Schlatter & Örlü 2010; Segalini et al. 2011). More importantly, the increase of the Reynolds number allows us to gain important insights in the turbulent dynamics, revealing important features, such as intermittency (Benzi et al. 1993; Frisch 1996; Biferale & Toschi 2001), the presence of coherent structures (Del Álamo et al. 2006) and interactions among the different scales of the flow (Hoyas & Jiménez 2006; Mathis et al. 2011).

In the spirit of the discussion above, in this thesis we aim at studying the turbulent dynamics in the presence of rotation and stratification by means of high-resolution numerical simulations. Such conditions are very important, especially in a geophysical perspective. A thorough understanding of turbulent processes should mainly focus on how energy is exchanged among different scales. This is important both from a scientific and a practical point of view. Critical evaluations as well as related improvements of large-scale atmospheric and oceanic models cannot be achieved unless the physics and the main mechanisms underlying atmospheric and oceanic dynamics are understood. In chapter 2, a short survey of the background on turbulence strongly affected by rotation and stratification is given. Chapter 3 presents a short overview on wall-bounded turbulence and on the effect of system rotation and stable stratification. In chapter 4, a summary of the main findings is offered. Finally, chapter 5 concludes with some general remarks and outlooks.

²defined as $Re_{\tau} = u_{\tau}L/\nu$. $u_{\tau} = \sqrt{\tau_w/\rho}$ is the friction velocity with τ_w being the shear stress at the wall.

³defined as $\int_0^\infty \left(1 - \frac{u}{U_\infty}\right) \frac{u}{U_\infty} dy$.

CHAPTER 2

Rotating and stratified turbulence: a geophysical perspective

Atmospheric and oceanic flows are highly affected by both rotation and stratification. Rotation is exerted through Coriolis forces which mainly act in horizontal planes whereas stratification largely affects the motion along the vertical direction through the Archimede's force. Depending on the mean density profile, stratification can either enhance or suppress vertical motions. Stratification in the atmosphere is usually stable above the boundary layer (Vallis 2006; Gill 1982), i.e. a fluid particle which is displaced in the vertical direction tends to return to its initial position. Whereas highly rotating flows tend to form structures which are elongated in the vertical direction (Taylor 1923), highly stratified flows favour thin structures elongated in the horizontal direction. Such structures are usually referred to as pancake structures (Lindborg 2006; Brethouwer et al. 2007). It is the interplay between these two regimes that gives rise to the variety of dynamics seen in the atmosphere.

In the most general case, the governing equations for the flows in the atmosphere and in the oceans are the compressible Navier-Stokes equations. Fluid density may change from place to place, affected by other scalar quantities such as pressure, temperature, humidity and salinity. Nevertheless, a good insight into the turbulent dynamics can be gained by reducing the complexity of the problem by making a few assumptions. Following the standard derivation, we restrict ourselves to the incompressible Navier-Stokes equations under the Boussinesq approximation on a f-plane. These can be written as

$$\frac{D\boldsymbol{u}}{Dt} = -\frac{\nabla p}{\rho_0} - f\boldsymbol{e}_z \times \boldsymbol{u} + b\boldsymbol{e}_z, \qquad (2.1a)$$

$$\frac{Db}{Dt} = -N^2 w, \qquad (2.1b)$$

$$\nabla \cdot \boldsymbol{u} = 0, \qquad (2.1c)$$

$$\frac{Db}{Dt} = -N^2 w, (2.1b)$$

$$\nabla \cdot \boldsymbol{u} = 0, \tag{2.1c}$$

where \boldsymbol{u} is the velocity vector, $f = 2\Omega$ is the Coriolis parameter with Ω being the rotation rate in the f-plane, e_z is the vertical unit vector, p is the pressure and D/Dt represents the material derivative. $N = \sqrt{g\rho_0^{-1}} d\bar{\rho}/dz$ is the Brunt-Väisälä frequency, with g being the gravity acceleration, ρ_0 a reference density and $d\overline{\rho}/dz$ the background density vertical gradient, and $b = g\rho/\rho_0$ is the buoyancy, where ρ is the fluctuating density. In general, b = b(T, S), where T

is the (potential) temperature and S the salinity. In the following, however, we will assume for simplicity that only T affects b and therefore that $b=gT/T_0$ (Vallis 2006). In (2.1) we have omitted diffusion terms which act only at very small scales. In the following sections, we simplify this system for the different atmospheric and oceanic regimes, shortly reviewing the main theories and the main open questions concerning turbulence in geophysical flows.

2.1. Geostrophic turbulence

Atmospheric and oceanic dynamics are forced at very large scales. In the atmosphere, available potential energy associated with the poleward temperature gradient is converted to kinetic energy by baroclinic instability which develops on scales of the order of thousand kilometres. The general circulation of the oceans is mainly driven by surface fluxes of momentum at similar spatial scales. At such large scales, Earth rotation strongly affects the flow. Moreover, the stratification is generally quite strong, both in the atmosphere and in the oceans (Pedlosky 1987; Vallis 2006).

The relative importance of Coriolis forces and buoyancy forces compared to inertial forces are often quantified by the Rossby and the Froude numbers, defined as

$$Ro = \frac{U}{fL}$$
 and $Fr = \frac{U}{NL}$. (2.2)

Here, L is a characteristic horizontal scale and U a characteristic velocity. Note that the use of a horizontal length scale rather than a vertical length scale in the definition of Fr is not standard in geophysical sciences (see e.g. Gill 1982). However, as will be discussed in the following, recent advancements in the understanding of stratified turbulence suggest that the Froude number defined with a vertical length scale always remains of the order of unity, even in strongly stratified regimes (Billant & Chomaz 2001). On the other hand, Fr, defined as in (2.2), is in most geophysical applications a small parameter. In the atmosphere, typical values of Fr are of the order of 10^{-3} and typical values of Ro are of the order of 10^{-1} (Deusebio et al. 2013b). Thus, in equations (2.1) the horizontal pressure gradient is mainly balanced by Coriolis forces (geostrophic balance), whereas the vertical pressure gradient is mainly balanced by buoyancy forces (hydrostatic balance).

For strong rotation rates, an asymptotic analysis with Ro as a small parameter is possible. For the details of such a derivation, we refer the reader to any geophysical fluid dynamic textbook, such as Vallis (2006) or Pedlosky (1987). At zero order, the velocity field, u_0 , is perfectly horizontal, divergence-free and in geostrophic balance. At first order in Ro, material conservation of the Charney potential vorticity (Charney 1971),

$$q_0 = -\frac{\partial u_0}{\partial y} + \frac{\partial v_0}{\partial x} + \frac{f}{N^2} \frac{\partial b_0}{\partial z}, \qquad (2.3)$$

is satisfied, i.e.

$$\frac{Dq_0}{Dt} = 0, (2.4)$$

where the material derivative retains only the horizontal advection contributions. In the following the subscript "0" will be dropped, for simplicity. Assuming hydrostatic balance and rescaling the vertical coordinates with f/N, it is possible to rewrite q in terms of the stream function¹, ψ , as $q = \nabla^2 \psi$. In the literature, equation (2.4) is often referred to as the quasi-geostrophic (QG) equation. The zero order expansion also conserves energy, that is

$$\frac{DE}{Dt} = -\nabla \cdot (p\boldsymbol{u}), \qquad (2.5)$$

where $E = (u^2 + v^2 + N^{-2}b^2)/2$. Therefore, the QG equation conserves independently two quadratic quantities, energy and potential enstrophy, where the latter is defined as half of the square of potential vorticity, $q^2/2$.

The energy and enstrophy wave number spectra, $E({\pmb k})$ and $Z({\pmb k}),$ are related as

$$E(\mathbf{k}) = k^{-2} \cdot Z(\mathbf{k}), \tag{2.6}$$

where k is the modulus of the three-dimensional wave-vector k, whereas E(k) and Z(k) are the energy and enstrophy content in mode k, respectively. This distinctive property of the QG equation, also shared with strictly two-dimensional flows, is the basis of its most interesting feature: the inverse energy cascade. As shown in a visionary paper of Kraichnan (1967), the presence of two related quadratic invariants in two-dimensional flows leads to a global energy transfer towards large scales, as opposed to three-dimensional flows in which energy is transferred towards small scales. Enstrophy, on the other hand, is transferred towards small scales in a forward cascade.

As shown in figure 2.1, if energy and enstrophy are injected at a scale k_f , energy cascades upscale in the energy inertial range whereas enstrophy is transferred downscale in the enstrophy inertial range. Following similar arguments as Kolmogorov (1941a), Kraichnan (1967) argued that inertial range statistics at a particular scale $l=2\pi/k$ are universal and do not depend on the viscosity ν . In the energy inertial range they only depend on the upscale flux of energy, ε . Simple dimensional considerations suggest a scaling for the energy spectrum as

$$E(k) = \mathcal{K}\varepsilon^{2/3}k^{-5/3}. (2.7)$$

Note that such an expression is similar to the one derived by Kolmogorov (1941a). However, the direction of the energy transfer is different, downscale in three-dimensional turbulence and upscale in two-dimensional turbulence. In a similar way, assuming that the statistics in the enstrophy range have a universal form which only depends on the enstrophy small-scale dissipation

¹being the zero order divergence free, the stream function $u_h = \nabla \times \psi e_z$ completely define the horizontal velocity.

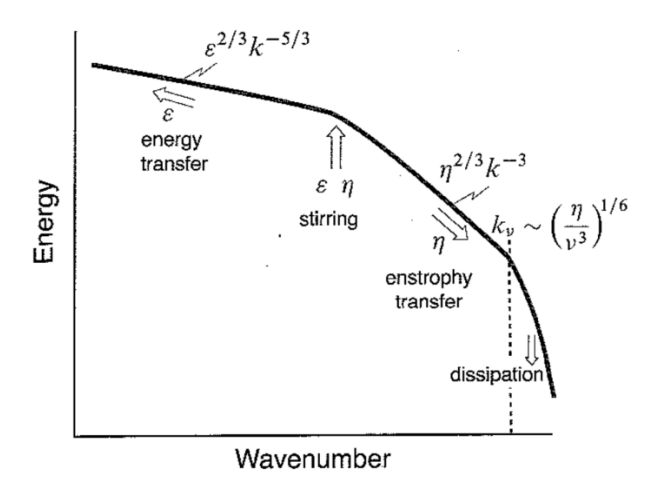


FIGURE 2.1. Sketch of the energy spectrum in twodimensional and in QG turbulence (figure taken from Vallis 2006).

leads to an energy spectrum of the form

$$E(k) = \mathcal{C}\eta^{2/3}k^{-3}. (2.8)$$

The dimensionless constants, \mathcal{K} and \mathcal{C} , are assumed to be universal and are often referred as Kraichnan and Kraichnan-Batchelor constant, respectively. The theory of Kraichnan (1967) has been tested numerically in a number of studies. Early investigations (Legras et al. 1988; Ohkitani 1990; Maltrud & Vallis 1993; Ohkitani & Kida 1992) indicated that the energy spectrum may be steeper in the enstrophy range as compared to Kraichnan's prediction. However, as computational resources allowed larger resolutions, (2.8) was recovered (Boffetta 2007; Vallgren & Lindborg 2011). As for the enstrophy inertial range, recent high-resolution numerical simulations have confirmed the existence of an inverse energy cascade, even though a somewhat steeper spectrum than (2.7) has been obtained by some investigators. This steeper spectrum is likely to be a result of formation of large scale coherent vortices (Scott 2007; Vallgren 2011).

To what extent can the theory of QG turbulence explain large-scale atmospheric and oceanic dynamics? Indeed, the inverse energy cascade of QG flows poses the question on how energy can be dissipated in rotating and stratified systems such as the Earth. Dissipation of kinetic and potential energy can only be achieved by means of molecular viscosity and diffusion which act at very small scales. In the atmosphere, for instance, these scales can be estimated to be of the order of few centimetres or even millimetres. How to reconcile the picture of a large-scale inverse energy cascade dynamics with the presence of small scale dissipation is a problem that has become increasingly

important as the resolution of numerical models has increased. Since QG dynamics is not able to support a forward energy cascade, non-balanced motions, which do not satisfy the geostrophic and hydrostatic balance, must be taken into account. How energy can be transferred from balanced quasi-geostrophic motions to ageostrophic motions is a fundamental question that we attempt to answer by means of high-resolution numerical simulations in Paper I and II.

2.2. Stratified turbulence

As flow scales decrease, the effects of rotation and stratification are reduced. In the atmosphere rotation becomes of secondary importance at scales of the order of tens of kilometres. However, at such scales stratification is still very important and typical Froude numbers are very small.

In the last decade there has been important advances in the understanding of turbulence in the presence of strong stratification. Thanks to novel numerical experiments it has been possible to resolve the issue regarding the direction of the energy cascade in the strongly stratified regime. In the early works it was suggested that strong stratification favours an inverse energy cascade. By rescaling the equations of motions as done by Riley et al. (1981), Lilly (1983) argued that strong stratification leads to the suppression of vertical motions and a two-dimensionalisation of the flow. In this limit, an inverse cascade would therefore be observed, as predicted by Kraichnan (1967). Lilly (1983) suggested that in the atmosphere energy in decaying three-dimensional convective turbulent patches would, due to the effect of the stable stratification, be transferred upscale and feed the growth of two-dimensional structures.

Despite the appeal of such a theory, advances in the understanding of strongly stratified turbulence in the last decade have proved that Lilly's view is wrong. In the limit of zero Fr, Billant & Chomaz (2001) showed that the Navier-Stokes equations allow for self-similar solutions with a vertical length scale $l_z \sim U/N$, proposing an alternative scaling of the equations than the one used by Lilly (1983) and Riley et al. (1981). Introducing different vertical and horizontal length scales, l_z and l_h respectively, and using the assumption of hydrostatic balance, we can make the estimate: $b \sim U^2/l_z$ and $w \sim bU/N^2 l_h \sim U l_h F r^2/l_z$. Thus, the following scalings for the advective terms should hold

$$u\frac{\partial}{\partial x} \sim \frac{U}{l_h}, \qquad w\frac{\partial}{\partial z} \sim Fr^2 \frac{U l_h}{l_z^2} \sim \frac{U}{l_h} \frac{Fr^2}{\delta^2},$$
 (2.9)

where $\delta = l_z/l_h$. Thus, if the estimate of Billant & Chomaz (2001) is used for l_z , it follows that $Fr \sim \delta$ and the vertical component of the advective term is of leading order and cannot be neglected as done in the analysis of Lilly (1983) and Riley et al. (1981). Billant & Chomaz (2001) introduced two different Froude numbers in their analysis, F_h and F_v , based on the horizontal and vertical length scales. Whereas F_h is a small quantity in strongly stratified turbulent flows, F_v always stays on the order of unity.

Thus, a stratified system retains its intrinsic three-dimensionality and never approaches the two-dimensional manifold. Moreover, Billant & Chomaz (2000) showed that in stratified flows two-dimensional solutions are unstable with respect to a new type of instability, called the zig-zag instability, and therefore tend to become three-dimensional (Augier et al. 2013). The theoretical findings of Billant & Chomaz (2001) have recently been confirmed in a number of numerical studies (Riley & deBruynKops 2003; Lindborg 2006; Waite & Bartello 2006; Brethouwer et al. 2007; Augier et al. 2012). Riley & deBruynKops (2003) studied the decaying of Taylor-Green vortices numerically in strongly stratified mediums. They found that the suppression of vertical motions induced by the stable stratification provides a decoupling of layers, leading to large vertical gradients. From an initial condition where $F_v \ll 1$, F_v increases and becomes of the order of unity, allowing for Kelvin-Helmotz instabilities (KH) to develop. Indeed, KH provides a physical mechanism which allows for a transfer of energy downscale. Also box simulations of forced strongly stratified turbulence have confirmed that stratification favours a direct cascade (Lindborg 2006; Waite & Bartello 2006; Brethouwer et al. 2007). In agreement with the prediction of Lindborg (2006), the two-dimensional horizontal kinetic and potential energy spectra in the inertial range are found to scale as $\,$

$$E_K(k_h) = C_1 \varepsilon_K^{2/3} k_h^{-5/3}, \qquad E_P(k_h) = C_2 \varepsilon_P k_h^{-5/3} / \varepsilon_K^{1/3},$$
 (2.10)

where ε_K and ε_P represent the kinetic and potential energy dissipation. C_1 and C_2 are found to be of the order of unity and have similar values, *i.e.* $C_1 \approx C_2 = 0.51 \pm 0.02$ (Lindborg 2006). Using dimensional arguments, Billant & Chomaz (2001) suggested a scaling for the vertical energy spectrum

$$E(k_z) = C N^3 k_z^{-3}, (2.11)$$

with the dimensionless constant C being of the order of unity. As noted by Brethouwer $et\ al.\ (2007)$, numerical and also experimental investigations of stratified turbulence are very demanding in terms of Reynolds numbers. It is only very recently that computational power has become strong enough to recover (2.11) in numerical simulations (Augier $et\ al.\ 2012$). In the inertial range of the turbulent cascade, the effect of viscosity is supposedly negligible. However, at moderate Reynolds numbers, the constraint on the vertical length scale due to stratification leads to severe limitations. The viscous term related to the second order vertical derivative can be estimated as

$$\nu \frac{\partial^2}{\partial z^2} u_i \sim \nu \frac{U}{l_z^2} \sim \nu \frac{U^2}{l_h} \frac{Re}{\delta} = \frac{U^2}{l_h} \frac{1}{Re \, Fr^2} \,, \tag{2.12}$$

which shows that the effective Reynolds number in stratified flows is reduced by a factor Fr^2 . Thus, even though Re is large, viscosity may affect the dynamics if stratification is very strong.

2.3. Three-dimensional turbulence

As the scales of the flow reduce even further, also stratification becomes of minor importance and classical three-dimensional Kolmogorov turbulence is recovered. The transition between these two regimes is usually assumed to be the so-called Ozmidov length scale, defined as (Ozmidov 1965)

$$l_O = \frac{\varepsilon^{1/2}}{N^{3/2}},\tag{2.13}$$

where ε is the energy flux towards small scales. The Ozmidov length scale is usually interpreted as the largest scale at which overturning motions are possible. Indeed, numerical simulations indicate that $k_O = 2\pi/l_O$ is the wave number at which the energy spectrum shows a transition from a k^{-3} dependence, relation (2.11), to a $k^{-5/3}$ dependence (Augier *et al.* 2012). Using the estimates of Billant & Chomaz (2001) and the estimate $l_h \sim u^3/\varepsilon$ (Lindborg 2006), the following relations can be derived,

$$\frac{l_h}{l_O} \sim Fr^{-3/2}$$
 and $\frac{l_z}{l_O} \sim Fr^{-1/2}$. (2.14)

The Ozmidoz length scale in the oceans has been estimated to be of the order of metres (Gargett $et\ al.\ 1981$), whereas in the atmosphere, typical values may vary between one metre, in strongly stratified atmospheric boundary layers (Frehlich $et\ al.\ 2008$), and ten metres, in the upper troposphere (Lindborg 2006). At smaller scales, classical three dimensional turbulence develops and the Kolmogorov (1941a) theory is valid. Vertical and horizontal energy spectra scale as

$$E(k) = C\varepsilon^{2/3}k^{-5/3}, (2.15)$$

with a direct energy cascade from large to small scales. The Kolmogorov constant, $C \approx 1.6$, is of the order of unity (Grant *et al.* 1962; Kaneda *et al.* 2003). Viscosity becomes important only at scales of the order of centimetres or even millimetres, where dissipation takes place.

2.4. Rotating turbulence

Even though rotating turbulence often appears in geophysical flows coupled to stratification, understanding how system rotation alone modifies the turbulent dynamics is very important. Rotating turbulence has been the subject of a vast number of studies in the literature (e.g. Ibbetson & Tritton 1975; Cambon et al. 1997; Smith & Waleffe 1999; Moisy et al. 2011). Besides the geophysical context, rotating turbulent also arises in a series of engineering problems, e.g. turbo-machinery. One of the most interesting features of flows subjected to system rotation is the presence of structures which are highly elongated in the direction of the rotation vector Ω (Taylor 1923; Hopfinger et al. 1982; Bartello et al. 1994; Davidson et al. 2006). In the following, we will assume that Ω is aligned with the vertical axis z. If the rotation is strong, the leading-order balance in equation (2.1) is between the Coriolis term and the pressure gradient. The vertical component of the curl of (2.1) reduces to

$$f\nabla_h \cdot \boldsymbol{u} = f\left(\frac{\partial u}{\partial x} + \frac{\partial v}{\partial y}\right) = -f\frac{\partial w}{\partial z} = 0,$$
 (2.16)

where ∇_h is the horizontal divergence operator. If we further assume that there is hydrostatic balance in the vertical direction, e.g. balance between the pressure term $\rho^{-1}\partial p/\partial z$ and the gravitational acceleration g, we find that also the vertical derivatives of u and v vanish in a constant density fluid. This is commonly referred to as Taylor-Proudman effect (Proudman 1916; Taylor 1923).

In a slightly weaker form, the Taylor-Proudman effect means that rotating flows are strongly anisotropic and exhibit very weak vertical gradients, *i.e.* vertically elongated structures develop. Columnar vortices have been observed in a number of experiments (Hopfinger *et al.* 1982; Davidson *et al.* 2006), even though the mechanisms underlying their formation are yet not fully understood (Waleffe 1993; Staplehurst *et al.* 2008). Davidson *et al.* (2006) show that elongated structures grow in the vertical from an initial state of decaying three-dimensional turbulence when system rotation is applied. The growth rate of the vertical integral length scale was found to be proportional to the rotation rate, $l_z \sim \Omega t$, suggesting that linear inertial wave can have a role on the formation process of columnar structures (Staplehurst *et al.* 2008).

Indeed, waves are thought to have a crucial importance in the dynamics of strongly rotating flows (Waleffe 1993; Embid & Majda 1998). However, linear mechanisms cannot explain the transfer of energy towards large scales and the growth of the vertical integral length scale, which is an intrinsically nonlinear phenomenon. The two-time scale analysis of Embid & Majda (1998) suggests that, at large rotation rates, transfer of energy among scales is dominated by triadic interactions of resonant waves (Waleffe 1993). Resonance takes place between three inertial waves which satisfy

$$\mathbf{k}_1 + \mathbf{k}_2 + \mathbf{k}_3 = 0$$
 and $\omega_1 + \omega_2 + \omega_3 = 0$, (2.17)

where \boldsymbol{k}_i is the wave vector and $\omega_i = f k_{z,i}/|\boldsymbol{k}_i|$ is the frequency of the ith inertial wave. Cambon et al. (1997) showed that transfer of energy tends to concentrate energy close to the plane $k_z = 0$ (as also suggested by the instability hypothesis of Waleffe 1993). This means that vertically elongated structures develop. Modes belonging to the plane $k_z = 0$, for which $\omega = 0$, constitute, however, a closed resonant-set, meaning that energy into/out of the $k_z = 0$ plane can only be transferred through off-resonant triad interactions (Waleffe 1993). An intriguing question is whether purely 2D dynamics with an inverse energy cascade would be recovered as $Ro \rightarrow 0$ (Chen et al. 2005). It is thought that two-dimensionalisation of the flow takes place through quasiresonant triads, for which (2.17) is approximately satisfied only to a certain degree (Cambon et al. 1997). On the other hand, it is worth pointing out that the analysis of Embid & Majda (1998) is built on the assumption that two separate time-scales exist in the flow: a slow advection time scale $t_a \sim L/U$, and a fast rotational time scale $t_w \sim \omega = f k_{z,i}/|\mathbf{k}_i|$, for which $t_w \ll t_a$. However, as $k_z \to 0$, the two time scales become similar and the analysis of Embid & Majda (1998) is likely to breakdown at $k_z/k_h \approx u/l_h f = Ro$ (Bellet et al. 2006), similar to what observed in stratified turbulence (Lindborg & Brethouwer 2007) where a traditional two time-scales analysis breaks down at $k_h/k_z \sim U/(Nl_h) = Fr$.

The fact that vertically-elongated structures develop in rotating flows poses severe limitations on experimental and numerical investigations of such a regime. Boundary layer dynamics at solid walls together with the vertical experimental confinement influence experiments conducted in rotating tanks (Ibbetson & Tritton 1975; Hopfinger & van Heijst 1993; Morize & Moisy 2006). In a similar way, numerical simulations can be affected by the choice of the vertical size of the computational domain, L_z . Numerical codes generally use periodic boundary conditions in all three directions. The finite box height limits the lowest wave number which can be represented, $\tilde{k}=2\pi/L_z$. Confining L_z therefore prevents energy to be transferred to wave numbers that are smaller than \tilde{k} . Recent studies of non-rotating unstratified turbulence have shown an interestingly dynamics when the vertical size of the computational domain is reduced, where features of 3D and 2D turbulent dynamics mix and superimpose (Celani et al. 2010). How this picture would change in the presence of a system rotation is the subject of Paper IV.

2.4.1. Symmetry breaking in rotating flows

One intriguing aspect of rotating flows is that the Coriolis term breaks the reflectional invariance of the Navier-Stokes equations. A quantity is said to be reflectional invariant if it does not change under transformations which flip the direction of one axis, e.g.

$$(x', y', z') \to (x, y, -z).$$
 (2.18)

Vectorial quantities should be referred to the appropriate system of reference, e.g.

$$(u', v', w') \to (u, v, -w).$$
 (2.19)

Equations (2.1) are clearly not invariant with respect to the transformation (2.18) and (2.19), because of the Coriolis term. As a consequence, positive and negative vortical motions exhibit different properties in rotating flows. Experiments in rotating tanks of barotropic vortices show completely different flow evolution and patterns depending on the sign of the vorticity (van Heijst & Kloosterziel 1989; Hopfinger & van Heijst 1993). Motions with a positive vorticity with respect to the direction of the rotation vector are referred to as cyclonic, whereas motions with a negative vorticity are referred to as anticyclonic. A dominance of cyclonic motions has been observed in a number of studies of rotating turbulence, both in numerical simulations (Bartello et al. 1994; Smith & Waleffe 1999) and experiments (Hopfinger et al. 1982; Moisy et al. 2011). One way of quantifying the breaking of symmetry is by means of the skewness of the vorticity component parallel to the rotation rate vector (Bartello et al. 1994):

$$S(\omega_z) = \frac{\langle \omega_z^3 \rangle}{\langle \omega_z^2 \rangle^{3/2}}.$$
 (2.20)

Gence & Frick (2001) showed that, if rotation is applied to a fully developed isotropic three-dimensional turbulence, the numerator $\langle \omega_z^3 \rangle$ has a positive growth in time, thus giving evidence of a dominance of cyclonic motions during the transient spin-up process. Stability analysis may also provide an indication of the dominance of cyclonic motions. The inviscid Rayleigh criterion in an inertial frame of reference suggests that barotropic cyclonic vortices are more stable than their anti-cyclonic counterparts, in agreement with the observations (Kloosterziel & van Heijst 1991). Sreenivasan & Davidson (2008) also found that the Ro threshold for blobs to evolve into columnar vortices is lower for anti-cyclonic motions, which are thus less likely to appear.

Even though several explanations have been proposed for the dominance of cyclonic motions and this subject has been the object of an increasing attention in recent years, the understanding of the symmetry breaking in rotating turbulence is just "little more than a superficial cartoon" (Davidson et al. 2012). An intriguing question also concerns the limit of very strong rotation and stratification, discussed in §2.1. In this limit the Navier-Stokes equations reduce to the QG equation, (2.4), which, interestingly, is parity-invariant. Thus, in the QG limit there can be no cyclonic/anti-cyclonic symmetry breaking.

Even though we are not able to offer a new explanation in this thesis, we anyway address the symmetry breaking in rotating turbulence in Paper III and IV. We propose the use of an another quantity which may be of interest in place of ω_z , that is the statistics of the azimuthal velocity difference $\delta u_T = \mathbf{t} \cdot (\mathbf{u} (\mathbf{x} + \mathbf{r}) - \mathbf{u} (\mathbf{x}))$, where \mathbf{t} is an horizontal unit vector perpendicular to the separation vector \mathbf{r} in the cyclonic direction. ω_z is in fact a small-scale quantity in three-dimensional turbulence, meaning that its value is dominated by contributions at small-scales, and therefore a measure based on (2.20) may be Re-dependent. On the other hand, statistics of δu_T retain the dependence on the separation scale \mathbf{r} and can thus be more informative.

2.5. Towards the atmosphere...

Even though the separate turbulent regimes (three-dimensional, stratified and geophysical turbulence) have been widely studied in the last decade, investigations of the transition from one dynamics to another are rather scarce. Indeed, within the context of numerical simulations, the available computational resources impose severe constraints on the scale separations, and simulating more than one regime has not been possible until very recently.

In order to shed light on atmospheric and oceanic dynamics, such investigations are very important. One issue which is still an object of a vivid debate is the so-called Nastom-Gage spectrum. By using sensors mounted in commercial aircraft, Nastrom et al. (1984) were able to measure the kinetic and potential energy spectra in the atmosphere from scales of the order of few kilometres up to scales of the order of thousand kilometres. The striking outcome of their work was the observation that the atmospheric energy spectrum clearly divides into two separate regimes (see figure 2.2): at synoptic scales ($\sim 1000 \text{ km}$) a

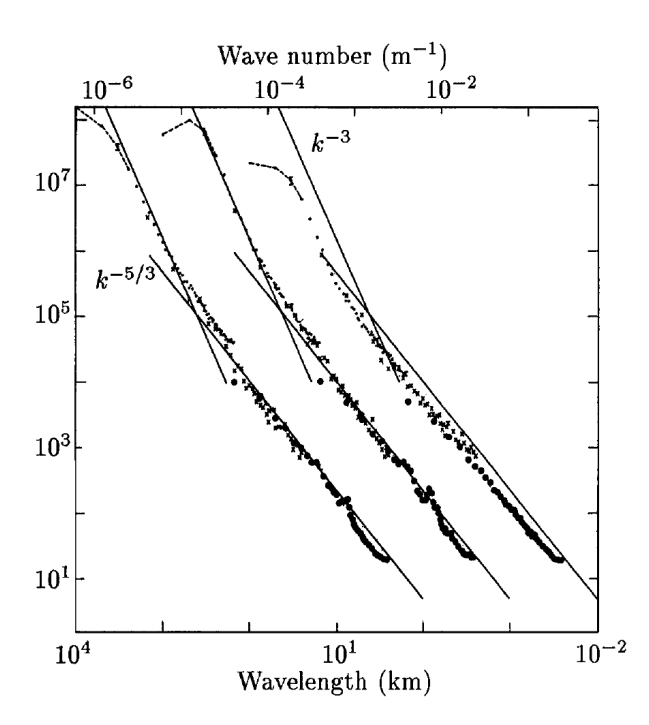


FIGURE 2.2. Atmospheric spectra of kinetic energy of the zonal and meridional wind components and potential energy measured by means of the potential temperature. The spectra of meridional wind and potential temperature are shifted one and two decades to the right, respectively. Reproduced from Nastrom & Gage (1985).

spectrum of the form $\sim k^{-3}$ is found, whereas at mesoscales (~ 100 km) much shallower spectra are observed, $\sim k^{-5/3}$, with a smooth transition around 500 km. More than twenty-five years later, it is still debated what dynamics are producing these spectra.

While the k^{-3} range can be explained by a quasi-geostrophic turbulent dynamics, the $k^{-5/3}$ range is more mysterious and intriguing, since such a spectrum may arise from both stratified and geostrophic turbulence (Vallis 2006). However, the underlying dynamics is completely different in the two cases, with a downscale cascade of energy in the former case and an upscale cascade of energy in the latter case. Early studies, e.g. Lilly (1983), interpreted the $k^{-5/3}$ range as a stratified upscale energy cascade. Nevertheless, recent progress in stratified turbulence theory rather suggests that the $k^{-5/3}$ range is a result of a downscale energy cascade. In spite of this, Lilly's interpretation has recently been revived by some experiments in electromagnetically forced thick layers, suggesting that the presence of large-scale coherent vortices might suppress vertical motion and allow for an inverse cascade (Xia et al. 2011).

In order to determine the direction of the cascade in the $k^{-5/3}$ range, other statistical quantities can be used in place of the energy spectrum. One such quantity is the longitudinal third-order structure function,

$$\langle \delta u_L \delta \boldsymbol{u} \cdot \delta \boldsymbol{u} \rangle = \langle (u_L (\boldsymbol{x} + \boldsymbol{r}) - u_L (\boldsymbol{x}))$$

$$(\boldsymbol{u} (\boldsymbol{x} + \boldsymbol{r}) - \boldsymbol{u} (\boldsymbol{x})) \cdot (\boldsymbol{u} (\boldsymbol{x} + \boldsymbol{r}) - \boldsymbol{u} (\boldsymbol{x})) \rangle,$$
 (2.21)

where u_L is the velocity component parallel to \boldsymbol{r} and $\langle \cdot \rangle$ denotes the ensemble average. As opposed to the energy spectrum, the sign of $\langle \delta u_L \delta \boldsymbol{u} \cdot \delta \boldsymbol{u} \rangle$ differs depending on the direction of the cascade, and therefore has been used to study the atmospheric dynamics (Lindborg 1999; Cho & Lindborg 2001). In three-dimensional turbulence, an exact relation can be derived (Kolmogorov 1941b; Antonia et al. 1997),

$$\langle \delta u_L \delta \boldsymbol{u} \cdot \delta \boldsymbol{u} \rangle = -\frac{4}{3} \varepsilon_K r. \tag{2.22}$$

Its counterpart in two-dimensional turbulence was derived by Lindborg (1999) who found that $\langle \delta u_L \delta u \cdot \delta u \rangle$ is positive and has a cubic dependence in the enstrophy cascade range,

$$\langle \delta u_L \delta \boldsymbol{u} \cdot \delta \boldsymbol{u} \rangle = \frac{1}{4} \eta r^3,$$
 (2.23)

and a linear dependence in the energy cascade range,

$$\langle \delta u_L \delta \boldsymbol{u} \cdot \delta \boldsymbol{u} \rangle = 2Pr. \tag{2.24}$$

Here, η is the enstrophy dissipation and P the energy injection rate. Analyses of the third-order structure functions calculated from measurements in the lower stratosphere (Cho & Lindborg 2001) have shown a positive nearly-cubic dependence at large scales, and a negative linear dependence at small scales, supporting the idea of a direct cascade of energy. Moreover, by using (2.23) and (2.24), Cho & Lindborg (2001) estimated the downscale enstrophy and energy transfer², which were found to be of the order of $2 \times 10^{-15} \, \mathrm{s}^{-3}$ and $6 \times 10^{-5} \, \mathrm{m}^2 \, \mathrm{s}^{-2}$, respectively. However, it is questionable whether the use of (2.23) and (2.24), which were derived in the context of two-dimensional turbulence, is justified, especially in the mesoscales. As suggested by the analysis of Billant & Chomaz (2001), vertical gradients may be important.

That the $k^{-5/3}$ range can be explained by a direct energy cascade poses the question where the energy feeding such a cascade could come from. As noted in the previous section, purely geostrophic dynamics is not consistent with a downscale energy transfer. In order to investigate such a process, high-resolution numerical simulations are needed, able to resolve both geostrophic and stratified turbulent dynamics. In the last decade, several numerical studies have been devoted to shed some lights into the dynamics, both using idealised box simulations (Kitamura & Matsuda 2006; Vallgren et al. 2011) and atmospheric models (Skamarock 2004; Takahashi et al. 2006; Hamilton et al. 2008; Waite & Snyder 2009).

 $^{^{2}}$ in equation (2.24) P is interpreted as the downscale energy flux

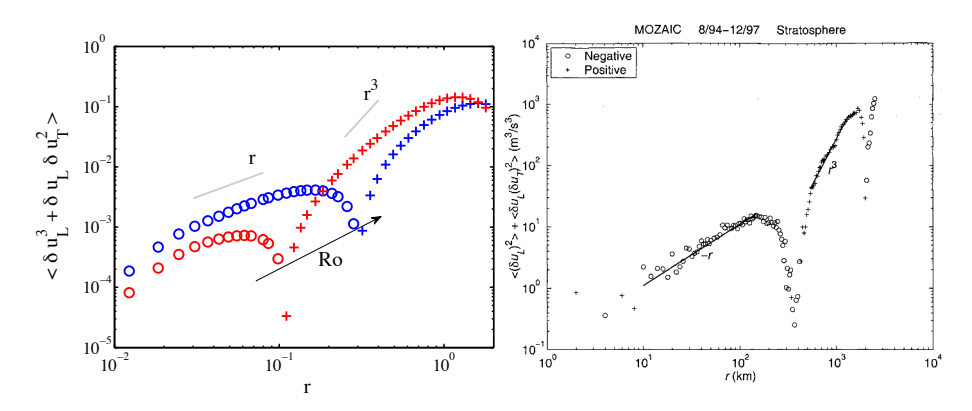


FIGURE 2.3. Comparison of the longitudial third-order structure function $\langle \delta u_L^3 + \delta u_L \delta u_T \rangle$ (left) from idealized geostrophic turbulence simulations (Vallgren et al. 2011) and (right) from measurements in the lower stratosphere (reproduced from Cho & Lindborg 2001). + Positive values and \circ negative values.

In paper I, II and III, we propose a possible interpretation of the largescale turbulent dynamics in the atmosphere. Motivated by the robustness of the transition of the energy spectrum, somewhat independent of the location and altitude, we hypothesise that it must be generated by a strong physical mechanism. Thus, in order to investigate the underlying dynamics, we carry out idealised box-simulations of rotating and stratified turbulence forced only at large scales. As opposed to quasi-geostrophic dynamics, finite rotation rates lead to a finite downscale cascade of energy. The small scales dissipation is found to increase with increasing Ro. The energy cascade originates from the largest scales of the system but becomes visible only at small-scales, where it leads to a shallowing of the energy spectra to a $k^{-5/3}$ dependence, consistent with observations (Nastrom & Gage 1985). The third-order structure function $\langle \delta u_L^3 + \delta u_L \delta u_T^2 \rangle$, where u_T is the horizontal velocity component perpendicular to r, switches sign at the transition wave number (figure 2.3), in agreement with Cho & Lindborg (2001). Negative signs with a linear dependence are attained at small scales, confirming the presence of a direct cascade of kinetic energy. On the other hand, the longitudinal velocity-temperature-temperature structure function,

$$\langle \delta u_L \delta T^2 \rangle = \langle (u_L (\boldsymbol{x} + \boldsymbol{r}) - u_L (\boldsymbol{x})) \cdot (T (\boldsymbol{x} + \boldsymbol{r}) - T (\boldsymbol{x}))^2 \rangle,$$
 (2.25)

is always negative and shows a linear dependence in r, consistent with the findings of Lindborg & Cho (2000) in the atmosphere (figure 2.4). As already noted by Lindborg & Cho (2000), this result is surprisingly clean. In Paper III, we make the interpretation that this is an indication of a downscale cascade of potential energy and, from the measurements, we estimate the downscale potential energy flux, Π_P , in the stratosphere to be $2 \times 10^{-2} \,\mathrm{m}^2\mathrm{s}^{-3}$.

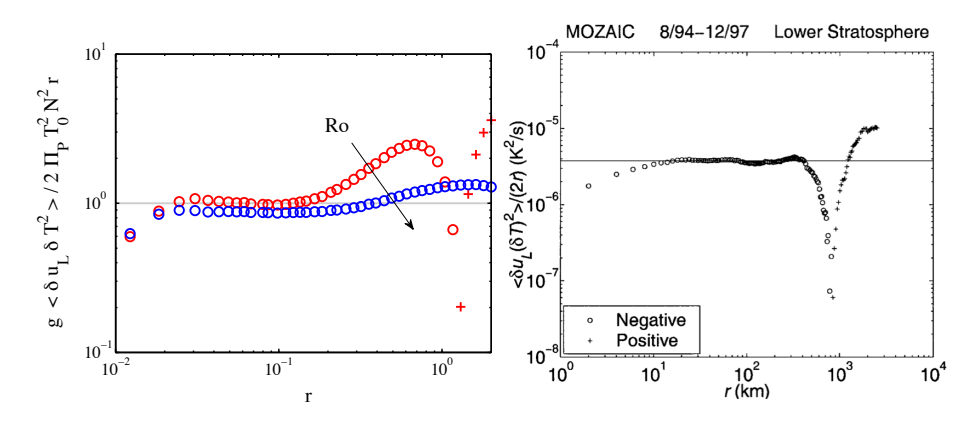


FIGURE 2.4. Comparison of the longitudial velocity-temperature-temperature third-order structure function $\langle \delta u_L \delta T^2 \rangle$ (left) from idealized geostrophic turbulence simulations and (right) from measurements in the lower stratosphere (reproduced from Lindborg & Cho 2001). + Positive values and \circ negative values.

CHAPTER 3

Stratified and rotating turbulence in the presence of walls

Most flows in engineering applications and in nature develop over surfaces. From a practical point of view, the study of turbulence in the vicinity of a solid wall is therefore of essential importance. Early experimental investigations (e.g. Reynolds 1886) were mainly devoted to wall-bounded turbulence. An inhomogeneous direction, normal to the wall¹, substantially increases the complexity of the problem, as compared to the homogeneous case. From a numerical point of view, more complex numerical schemes and discretisations are needed in order to deal with solid boundaries. It was only as late as in the end of the 80s that computational resources had reached a level that allowed for wall-bounded turbulence simulations.

3.1. The scales of motions in wall-bounded turbulence

As in the isotropic homogeneous case, turbulent flows over solid walls possess many scales. Figure 3.1 (taken from Deusebio et al. 2013a) shows a horizontal component of the velocity in a wall-parallel plane close to the wall (figure 3.1a) and far from the wall (figure 3.1b). The turbulent dynamics is highly inhomogeneous and very different patterns are observed depending on the distance from the wall. In closed flows, such as channel or pipe flows, the largest turbulent length scale is set by geometrical constraints, such as the channel height h or the pipe diameter d. In boundary layers, on the other hand, where the flow is bounded at one side only, the largest scales are rather set by the boundary layer thickness. Away from the surface (figure b), a multitude of eddies of different size can be observed, with small-scale structures embedded in larger structures. Turbulence is close to be homogeneous and energy containing eddies are much larger than the scale at which energy is dissipated, which is of the order of the local Kolmogorov length scale, $\eta = (\nu^3/\varepsilon)^{1/4}$. Here, ε is the local dissipation rate. On the other hand, figure 3.1b shows that close to the wall the dynamics is dominated by a population of streamwise-elongated regions of high and low velocity. These small-scale structures, which are often referred to as *streaks*, are common to all turbulent flows developing over a solid surface. Their size scales

¹hereafter denoted by y. The reader shall note that here we change the vertical axis from z to y in order to be consistent with the convention in wall-bounded turbulence studies, e.g. Spalart (1989).

with the local shear stress τ_w and the kinematic viscosity ν . Thus, energy-containing eddies and viscous scales coincide and no inertial range, as observed in three-dimensional turbulence, is observed very close to the wall. The length scale which can be formed from τ_w and ν ,

$$l^{+} = \nu \sqrt{\frac{\rho}{\tau_w}} = \frac{\nu}{u_{\tau}},\tag{3.1}$$

is often referred to as the viscous unit and $u_{\tau} = (\tau_w/\rho)^{1/2}$ is usually referred to as the friction velocity, which is the relevant reference velocity close to the wall. Streaks display a spanwise spacing of about $\approx 100\,l^+$, with remarkable agreement between different flows. The ratio between the largest turbulent length scale δ and the viscous scale l^+ is referred to as the friction Reynolds number,

$$Re_{\tau} = \frac{\delta}{l^{+}} = \frac{\delta u_{\tau}}{\nu}.$$
 (3.2)

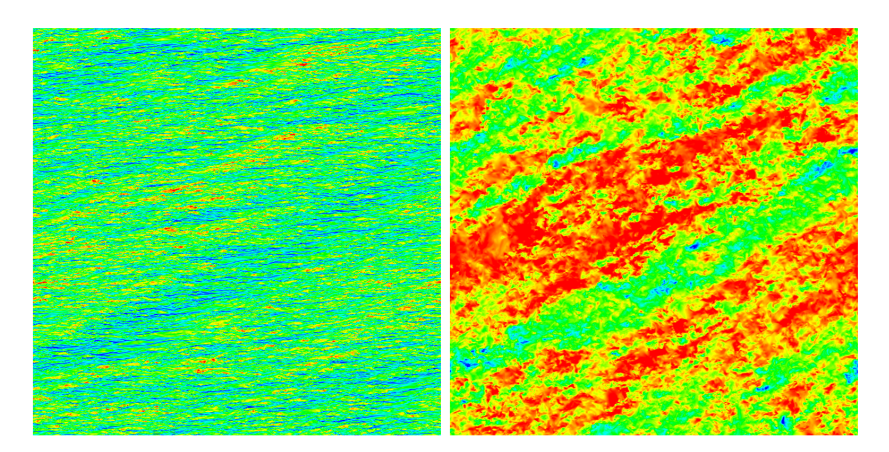


FIGURE 3.1. Horizontal component of the velocity parallel to the direction of the mean shear stress at the wall in a wall-parallel plane (taken from Deusebio *et al.* 2013*a*). *a)* Plane at $y^+ = y/l^+ = 12$ *b)* Plane at $y^+ = y/l^+ = 800$.

The fact that there are two widely separated length scales, l^+ close to the boundary and δ far from the boundary, is the foundation of the theory of inner and outer scaling (Millikan 1938; Townsend 1976). Turbulence statistics at wall distances comparable to δ are assumed to be universal and to scale with δ and the outer velocity U_{∞} (outer scaling). On the other hand, at distances comparable to the viscous unit l^+ , statistical quantities are assumed to scale with l^+ and u_{τ} (inner scaling). In the lower part of the inner region, $y < 5 \, l^+$, friction dominates and $du^+/dy^+ \approx 1$, where the superscript l^+ refers to a generic quantity normalised using inner scaling quantities. Thus, close to the wall velocity increases linearly with height, i.e. $u/u_{\tau} = y/l^+$. This layer is usually referred to as the viscous sub-layer. Above $y^+ \approx 5$, du^+/dy^+ is not of

the order of unity, although inner scaling still applies. This region is referred to as the buffer layer. The two scalings match in an intermediate region (Millikan 1938). In such a layer, the velocity gradient $\partial u/\partial y$ must become independent of ν and δ , and scale only with u_{τ} and the distance from the wall y, *i.e.* $\partial u/\partial y \sim u_{\tau}/y$. This leads to a logarithmic profile for the velocity,

$$u^{+} = \frac{1}{\kappa} \log y^{+} + C, \tag{3.3}$$

where κ is the von Kármán constant. Figure 3.2 shows a prototype of the horizontal velocity profile in wall-bounded flows. The different regions, viscous sub-layer, buffer layer, logarithmic region and outer layer can be observed. Ever since the discovery of the log-layer in wall-bounded flows, there has been a large debate concerning whether there exists a true constant κ which is universal to all wall-bounded flows. Indeed, results spanning several decades in Re numbers, ranging from experiments (Österlund et~al. 2000; Monkewitz et~al. 2007; Marusic et~al. 2010), numerical simulations (Hoyas & Jiménez 2006; Schlatter et~al. 2009; Spalart et~al. 2009) and measurements in the atmosphere (Businger et~al. 1971; Andreas et~al. 2006), have shown a relatively modest variation of κ , ranging from 0.35 to 0.42. It is worth pointing out that these references are not exhaustive and they are only a very small part of the vast number of studies aimed at determining κ . An accurate description of this layer is, in fact, of great practical interest, since most of the turbulent dissipation at high Re occurs in the log-layer.

Although the inner/outer scaling theory has been very successful in predicting mean profiles, its applicability to higher moments is more questionable. In figure 3.3, the horizontal and vertical fluctuations scaled by u_{τ}^2 are shown for several Re (Spalart et al. 2009; Deusebio et al. 2013a). Even very close to the wall, at $y^+ \approx 12$, the intensity of the near-wall peak located at $y^+ \approx 12$ does not collapse for the different Re and it clearly increases with Re, suggesting that there is a large-scale influence in the near-wall scaling. The variation of the maximum of u_{rms} with Re has received a great deal of attention in recent years and some empirical relations have been proposed, generally in the functional form of a logarithm (e.g. Marusic & Kunkel 2003). As shown by figure 3.1, footprints of the large-scale structures can be seen close to the wall, suggesting that the outer structures penetrate deeply into the boundary layer and affect the near-wall turbulence scaling. Several studies have focused on the interaction between large and small scales, involving spectral analysis (Hoyas & Jiménez 2006) as well as quantification of the small-scale modulations due to large scale structures (Schlatter & Örlü 2010; Mathis et al. 2011). In order to study such interactions a large separation of scales, and therefore a large Re. is desirable. Recent advancement in experimental techniques as well as new facilities able to achieve extremely high Re will therefore provide extremely valuable data needed to study the interaction between outer and inner scalings in wall-bounded flows (Hultmark et al. 2012; Marusic et al. 2013; Rosenberg et al. 2013).

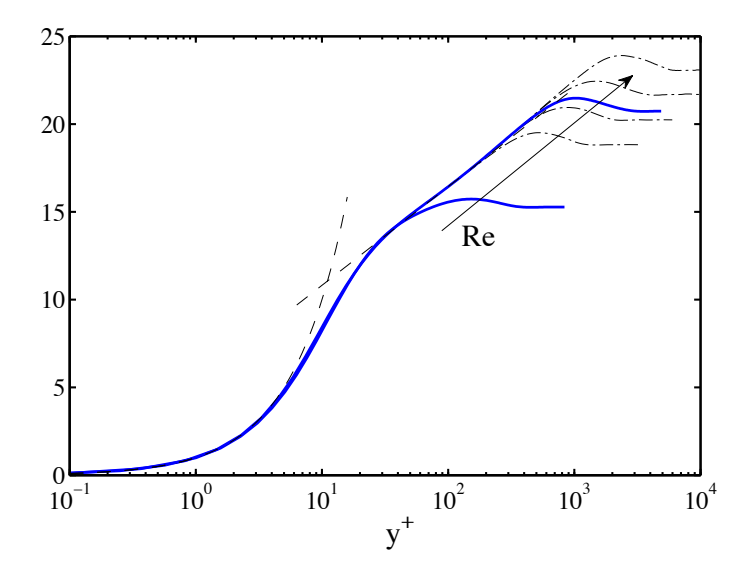


FIGURE 3.2. Total horizontal wind $\sqrt{\overline{u}^2 + \overline{w}^2}/u_{\tau}$ profile in viscous scaling. Thin lines represent the law of the wall $\overline{u}^+ = y^+$ and the logarithmic region $\overline{u}^+ = 1/0.41 \log y^+ + 5.5$. (thick) Deusebio *et al.* (2013*a*) at $Re = 400, 1600 - \cdots$ (thin) Spalart *et al.* (2009) at Re = 1000, 1414, 2000, 2828.

From a numerical point of view, an accurate simulation of turbulent flows should resolve all the turbulent scales, from the smallest to the largest. In wall-bounded flows, turbulent motions are naturally forced by the wall-normal mean shear. Kinetic energy is extracted from the mean flow and transferred to the turbulent field. One of the most interesting features of wall-bounded turbulence is that most of the turbulent kinetic energy is produced very close to the wall, at $y^+ \approx 12$, where velocity gradients are large (Pope 2000). Thus, unlike homogeneous turbulence, energy is injected at very small-scales. As a consequence small-scale dynamics is of primary importance in wall-bounded flows. How energy diffuses to larger scales, how outer structures interact with the near-wall structures and vice versa are problems that are not fully understood and whose understanding are crucial in order to improve turbulence modelling for wall-bounded flows (Jiménez 2012).

Whereas small-scale structures show very common characteristics among all wall-bounded flows, the large scales are, on the other hand, very sensitive to flow geometry. Therefore, there is no general rule that determines their size and one has to be very careful in choosing the dimension of the computational domain, which artificially confines the largest scales in a DNS. Convergence tests should always be performed in order to check the effects of changes in the domain size, although this may often become unfeasible as high Re are considered.

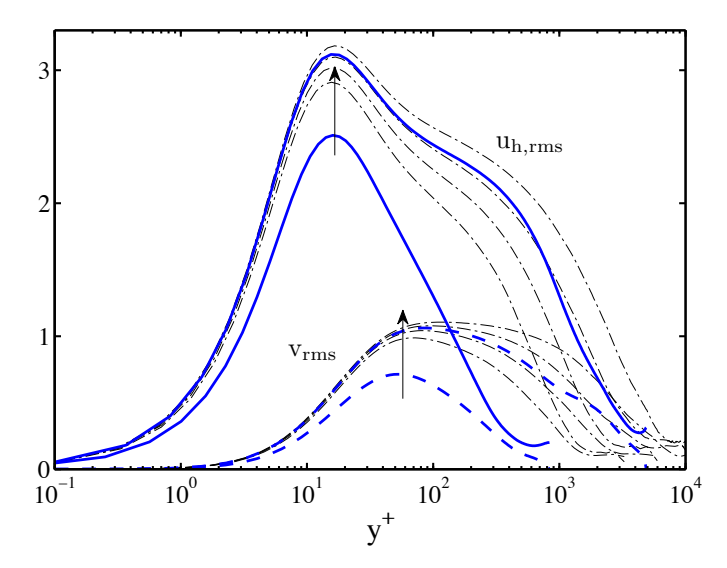


FIGURE 3.3. Total horizontal (——) $\sqrt{\overline{u'^2} + \overline{w'^2}}$ and vertical (---) $\sqrt{\overline{v'^2}}$ profiles scaled with u_{τ} . Lines as in figure 3.2. Arrows in the direction of increasing Re.

3.2. Numerical grids in wall-bounded flows

Since the first simulations in the 70s (Orszag & Patterson 1972), numerical simulations of turbulent flows have heavily relied on the use of spectral methods (Canuto et al. 1988). As opposed to finite difference methods (FD) where the solution is approximated on a finite grid, spectral methods (SM) approximate the solution by using an expansion of known globally-defined ansatz functions. Instead of solving for the values at the grid points, spectral methods solve for the expansion coefficients. The only approximation which is introduced is the truncation of the spectral expansion, whereas differential operators acting on the solution are exact. Due to the fact that a priori known functions are chosen, SM are not very flexible and only flows in fairly simple geometries can be studied. However, as compared to the algebraic convergence of the solution provided by finite difference methods, spectral methods allow for an exponential converge which had made them particularly useful, especially for turbulence simulations.

Several kind of ansatz functions can be used for the spectral expansion. The early studies of homogeneous isotropic turbulence (e.g. Orszag & Patterson 1972) widely employed Fourier modes. Apart from the existence of fast transform algorithms (Fast Fourier Transforms, hereafter FFTs), Fourier modes also have the advantage of allowing for very simple formulations of partial differential equations since they are the eigenfunctions of the differential operator.

However, for wall-bounded flows Fourier modes are not suitable in the wall-normal direction, due to the inhomogeneous boundary conditions and the need for a non-equispaced grid (since wall structures are much finer as compared to the outer ones). In the early numerical studies of wall-bounded turbulence, Chebyshev polynomials were instead used and applied to Gauss-Lobatto grids

$$y_j/L = \cos\left(\pi \frac{j-1}{N-1}\right) \qquad j = 1, \dots, N, \tag{3.4}$$

which allowed both to retain the use of FFTs and to provide a non-uniform distribution, with a clustering of points at the upper and lower boundaries, $y=\pm 1$. Such a grid is particularly suitable for flows confined by two solid walls, e.g. channel flows. However, if one aims at studying open flows which are bounded by only one solid wall, the clustering of points at the free-boundary is a waste.

One way to overcome this problem is to use the method of Spalart et al. (2008) who employed Jacobi polynomials in the variable $\zeta = \exp(-y/Y)$, i.e. in a vertical grid exponentially stretched by a factor Y. Hoyas & Jiménez (2006) employed seven-point compact finite differences in place of the Chebyshev polynomials. In this way, they were able to adapt the grid spacing to the local viscous length scale η . Nevertheless, the employed solution algorithm still imposes a clustering of points at the upper boundary. In paper VII, we propose an alternative method in order to study open flows which satisfy the upper boundary condition

$$\frac{\partial u}{\partial y} = \frac{\partial w}{\partial y} = v = 0, (3.5)$$

with u and w being the streamwise and spanwise velocities, respectively. We retain the use of Chebyshev polynomials and the use of Gauss-Lobatto grids. However, we recast the study of open flows by considering flows which possess symmetries around y=0. The free-shear condition, when applied at y=0, can in fact be viewed as a symmetric condition for u and w and an antisymmetric condition for v. Thus, we can use only even Chebyshev polynomials in the expansion of u and w, and only odd Chebyshev polynomials in the expansion of v. If vertical stratification is present, the scalar field must have the same parity of the v equation and must therefore be odd. The spacing of the Gauss-Lobatto grid at v = 0 is coarse and the clustering of points at the free-shear boundary, now at v = 0, is thus avoided.

3.3. Rotating wall-bounded flows

Wall-bounded flows subjected to rotation around the vertical axis are very important in a geophysical perspective. Indeed, the derivation of the solution of a laminar rotating boundary layer of V. W. Ekman (1905) was inspired by observations that in Arctic regions icebergs move with an angle of $30^{\circ}-40^{\circ}$ with respect to the geostrophic wind (Nansen 1905). Far from the solid boundary, the main balance in the Navier-Stokes equations is between the Coriolis term and the pressure gradient, leading to the geostrophic balance $-\nabla p = \rho f e_y \times G$.

Here, e_y is the wall-normal unit vector and G is the geostrophic wind vector. As the surface is approached, viscous shear stresses become of leading order. For a laminar parallel flow in steady conditions, the horizontal components of the Navier-Stokes equations reduce to

$$fw' = \nu \frac{\partial^2 u'}{\partial x^2}$$
 and $-fu' = \nu \frac{\partial^2 w'}{\partial z^2}$, (3.6)

where the prime ' indicates the fluctuation around the geosotrophic wind, u-G. If vanishing boundary conditions for the velocity u' are applied at infinity, i.e.

$$u', w' \to 0$$
 as $y \to \infty$, (3.7)

the system (3.6) admits self-similar solution with respect to the scaled vertical coordinate y/δ_E , where $\delta_E = \sqrt{2\nu/f}$. In his landmark paper, Ekman (1905) derived the solution to (3.6) and (3.7),

$$u' = G_x - e^{-y/\delta_E} \{ G_x \cos(y/\delta_E) - G_z \sin(y/\delta_E) \}$$

$$w' = G_z - e^{-y/\delta_E} \{ G_x \sin(y/\delta_E) + G_z \cos(y/\delta_E) \}.$$
(3.8)

Ekman's work (1905) had such an importance that boundary layers subjected to a rotation around the vertical axis are nowadays referred to as Ekman layers in his honour. One of the most interesting features of the Ekman layer, in contrast to non-rotating boundary layers, is that the wind direction varies with height. Figure 3.4 shows the odograph of the horizontal velocities, equation (3.8), which is usually referred to as the Ekman spiral. The wall shear-stress has an angle of 45° with respect to the geostrophic wind direction, consistent with the observation of Nansen (1905) that icebergs move in a direction which is neither aligned with the geostrophic wind nor the oceanic current. It is worth pointing out that the condition (3.7) is rather demanding, especially in numerical simulations and experiments where the flow is usually confined vertically by the height of the domain, L_y . By replacing the boundary conditions (3.7) with the free-shear condition (3.5), the solution to (3.6) has the form (Deusebio et al. 2013a)

$$u = +C_1 \cosh(y/\delta_E) + C_2 \sinh(y/\delta_E)$$

$$w = -C_2 \sinh(y/\delta_E) + C_1 \cosh(y/\delta_E),$$
(3.9)

where the coefficients C_1 and C_2 depend on the rescaled domain height, $\chi=$ L_y/δ_E , as

$$C_1 = \frac{-u_g \cosh \chi \cos \chi - w_g \sinh \chi \sin \chi}{\cosh^2 \chi \cos^2 \chi + \sinh^2 \chi \sin^2 \chi}$$
(3.10)

$$C_1 = \frac{-u_g \cosh \chi \cos \chi - w_g \sinh \chi \sin \chi}{\cosh^2 \chi \cos^2 \chi + \sinh^2 \chi \sin^2 \chi}$$

$$C_2 = \frac{+u_g \sinh \chi \sin \chi - w_g \cosh \chi \cos \chi}{\cosh^2 \chi \cos^2 \chi + \sinh^2 \chi \sin^2 \chi}.$$
(3.10)

As $\chi \to \infty$, solution (3.9) exponentially converges to the Ekman solution (3.8).

Flows are very rarely laminar, especially in the atmosphere where the Ekman Reynolds number, $Re_E = G\delta_E/\nu$, is of the order of 10⁶. As the flow becomes turbulent, the Ekman spiral tends to shrink in the direction perpendicular to the geostrophic wind and the angle α between the wall shear-stress

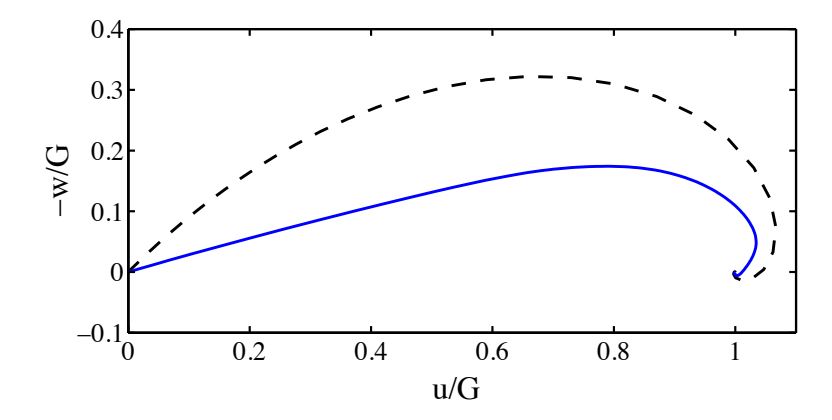


FIGURE 3.4. Ekman spiral for - - - a laminar Ekman boundary layer and —— a turbulent Ekman boundary layer.

and the geostrophic wind consequently reduces (figure 3.4) as an effect of the more efficient momentum transfer close to the wall (Coleman et al. 1990; Shingai & Kawamura 2002). Both in laminar and turbulent cases, the Ekman spiral shows a small overshoot of the geostrophic wind velocity at intermediate heights, which can also be observed in the maximum of the velocity profile shown in figure 3.2. This is usually referred to as the low-level jet. It should be pointed out that it does not originate from an excess of momentum which diffuses vertically, as in common jets, but rather arises as an effect of the system rotation.

An open question which is yet to be answered concerns the size and the nature of the largest structures of a turbulent Ekman boundary layer. In atmospheric boundary layers, large-scale structures have been observed and they are thought to be important on transport processes (Lemone 1973; Etling & Brown 1993). Experiments in a cylindrical annulus (Faller 1963; Faller & Kaylor 1966; Tatro & Mollo-Christensen 1966) have also shown that large-scale instabilities develop. Stability analysis of the laminar Ekman solution (3.8) shows that there are two kinds of instabilities: a viscous parallel instability appearing at $Re_E = 55$ and an inviscid instability arising for $Re_E > 115$ associated with inflectional points in the velocity profile (Faller & Kaylor 1966; Lilly 1966; Caldwell & Atta 1970). For both instabilities, the perturbation has the form of rolling structures which have a negative inclination, for the parallel instability, and a positive inclination, for the inviscid instability, with respect to the geostrophic wind (Lilly 1966). However, whether similar largescale structures are also present in turbulent flows is an open question. Early DNSs of turbulent Ekman layers at $Re_E = 400$ (Coleman et al. 1990) did not show any evidence of large-scale roll cells, unless convective motions driven by a moderate heating of the lower surface were present in the flow (Coleman et al. 1994). It is unclear whether the choice of the domain size may have prevented

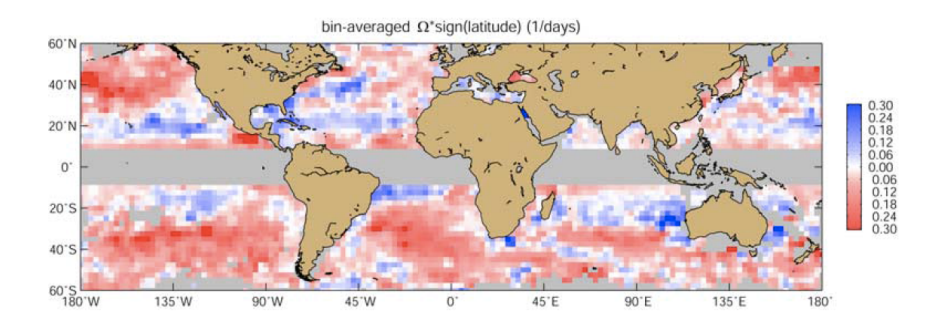


FIGURE 3.5. Average $5^{o} \times 5^{o}$ of the spin $\Omega \sim \omega_{y}/2$ (day⁻¹, with sign reversed in the Southern hemisphere): cyclones (anticyclones) are indicated by blue, positive values (red, negative values). Figure taken from Griffa *et al.* (2008).

their development. More recent flow visualisations of Ekman layers in DNSs at $Re_E=775$ indicate that there are large-scale structures which are not aligned with the direction of the geostrophic wind. Such structures were not observed in earlier DNSs (Shingai & Kawamura 2004). In paper V, we address the issue of large-scale structures in Ekman boundary layers at high Re_E .

Rotating boundary layers present interesting differences with respect to their non-rotating counterparts. As pointed out in §2.4.1, rotational terms break the parity invariance of the Navier-Stokes equations, as also observed from (3.6). Besides experiments and numerical simulations (see section §2.4.1), this symmetry breaking is also clearly seen in the large scale dynamics of the Earth atmosphere. Satellite images show that motions in low-pressure systems are preferentially counter-clockwise in the northern hemisphere and clock-wise in the southern hemisphere. Preference for cyclonic or anticyclonic motions is observed both in the atmosphere (Cho & Lindborg 2001) and in the oceans (see figure 3.5 taken from Griffa et al. 2008). However, it is not obvious that the breaking of reflectional symmetry observed in large-scales atmospheric dynamics can also be observed at smaller scales, for which Coriolis forces have a negligible effect. In this thesis, we present evidences that Ekman layers, in contrast to non-rotating boundary layers, can have a non-zero mean helicity and that a helicity cascade of a definite sign develops. We thus show that, as a consequence, the symmetry breaking can be observed down to the very smallest scales of motions, the Kolmogorov length scale η , which is of the order of one millimetre. Helicity, which is defined as the scalar product of velocity and vorticity

$$\mathcal{H} = \boldsymbol{u} \cdot \boldsymbol{\omega},\tag{3.12}$$

was first introduced by Moffatt (1969) who showed that it is an inviscidly conserved quantity in a barotropic fluid, *i.e.* for which $p = p(\rho)$. However, unlike energy and enstrophy, helicity does not have a definite sign and if the

equations satisfy reflectional symmetry, positive and negative helicity events occur with the same probability, leading to a zero mean helicity.

Because of its conservation property, helicity has historically aroused scientists curiosity, especially in the context of turbulence (Brissaudw et al. 1973). In geophysical applications, helicity is significant in tornados (Tsinober & Levich 1983; Lilly 1986) and is used to predict their development (Thompson 2005). Several studies have focused on understanding the helicity dynamics (Tsinober & Levich 1983; Chen et al. 2003; Mininni & Pouquet 2009) and how helicity affects the turbulent dynamics (Biferale et al. 2012). These studies exclusively focused on homogeneous turbulence. However, as shown in Paper VI, the presence of a wall is crucial for the generation of helicity in rotating flows. It can be easily shown that, unlike non-rotating boundary layers, the Ekman solution is helical (Zhemin & Rongsheng 1994). From the laminar solution (3.8), we find that

$$\mathcal{H} = G^2 \frac{e^{-2y/\delta_E}}{\delta_E} + G^2 \frac{e^{-y/\delta_E}}{\delta_E} \left(\sin \frac{y}{\delta_E} - \cos \frac{y}{\delta_E} \right), \tag{3.13}$$

is large and positive for $y < 3.94\delta_E$. In wall-bounded flows, being either laminar or turbulent, the injection of helicity is produced by the pressure gradient, $-\nabla p = 2\Omega e_y \times G$, which gives an overall injection of helicity over the entire boundary layer of (Deusebio & Lindborg 2013)

$$2\int_{0}^{\infty} \Omega \boldsymbol{e}_{y} \times \boldsymbol{G} \cdot \boldsymbol{\omega} dy = 2\Omega \int_{0}^{\infty} \boldsymbol{G} \cdot \frac{\partial \overline{\boldsymbol{u}}}{\partial y} dy = 2\Omega \boldsymbol{G} \cdot \boldsymbol{G}.$$
 (3.14)

The total injection can only be balanced by the mean and turbulent viscous helicity dissipation, ε_H and ε_h respectively,

$$\varepsilon_H = 2\nu \left(\frac{\mathrm{d}\overline{u}}{\mathrm{d}y} \frac{\mathrm{d}\overline{\omega_x}}{\mathrm{d}y} + \frac{\mathrm{d}\overline{w}}{\mathrm{d}y} \frac{\mathrm{d}\overline{\omega_z}}{\mathrm{d}y} \right) \qquad \varepsilon_h = 2\nu \frac{\overline{\partial u_i'}}{\partial x_k} \frac{\partial \omega_i'}{\partial x_k}. \tag{3.15}$$

Here, the bar denotes an ensemble average. Thus, helicity of a definite sign, injected at large scale, is transferred towards small scales, where it is ultimately dissipated. In paper VI, we study the helicity dynamics in a turbulent Ekman boundary layer, presenting evidences that there exists a helicity cascade in atmospheric boundary layers. This suggests that symmetry breaking in geophysical flows can be seen down to the smallest scale, i.e. the Kolmogorov length scale. Measurements in the atmosphere may also provide valuable data for studying the helicity dynamics at high Re.

3.4. Stratified wall-bounded flows

Turbulent dynamics close to the Earth surface influence the way heat, momentum, moisture and pollution are exchanged and mixed. The study of how stable stratification affects near-wall turbulence is crucial in order to understand how the atmospheric boundary layer dynamics change during nights with clear sky and/or in polar regions, when net radiative cooling at the ground is large with values of the order of $60\,\mathrm{Ws}^{-2}$ (Derbyshire 1999). Under these conditions, stable stratification significantly suppresses turbulent motions (figure 3.6). Mahrt

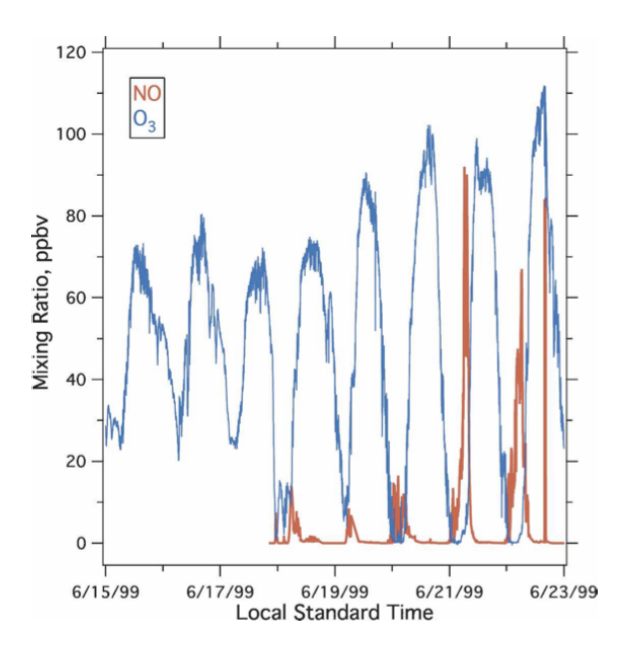


FIGURE 3.6. Figure taken from Banta *et al.* (2007). Time series of ground-level ozone (blue line, 1-min values in ppb) at Cornelia Fort Airpark, Nashville, Tennessee, for 15-22 Jul 1999 (times UTC). Daytime hours are marked by the maxima in O3 concentrations, and nights are the periods of mini- mum concentrations. NO measurements (red line, ppb) available after 17 Jun document local-source activity at this site at night.

(1998) divides the stable stratified boundary layer into two separate classes based on their phenomenological characteristics: the weakly stable boundary layer and the very stable boundary layer. The weakly stable boundary layer is relatively well understood and is characterized by continuous turbulence which is affected by buoyancy. On the other hand, the very stable boundary layer is somewhat more mysterious and less understood. Turbulence may be strongly damped and virtually absent (Zilitinkevich et al. 2008) and occasional bursts of turbulence can also be observed (Kondo et al. 1978). Atmospheric models need to be improved in order to take into account phenomena that arise in highly stably stratified conditions, as suppression of vertical motions, relaminarisation and appearance of gravity waves. Numerical simulations can provide an alternative tool, besides in-field measurements and experiments, to study the strongly stratified regime. This regime has recently been studied in a number of numerical investigations (e.g. Armenio & Sarkar 2002; Nieuwstadt 2005; Flores & Riley 2010; García-Villalba & del Álamo 2011; Deusebio et al. 2011).

For the weakly stable boundary layer, the so-called Monin-Obukhov similarity theory (Obukhov 1946; Monin & Obukhov 1954) has provided the foundation for our understanding of atmospheric flows, even for unstable stratification. The Monin-Obukhov similarity theory was introduced by Obukhov (1946) and Monin & Obukhov (1954) who proposed that in a region close to the surface, for which momentum and heat fluxes are approximately constant, statistical quantities are only functions of the distance y from the surface, the friction velocity u_{τ} , the wall heat flux q_w and the buoyancy parameter g/T_0 . Using Buckingham (1914)'s theorem, dimensionless quantities are thus functions of one independent dimensionless parameter: y/L, where L is the Monin-Obukhov length given by

$$L = -\frac{u_{\tau}^3 T_0}{\kappa g q_w}. (3.16)$$

The von Kármán constant κ is historically included in the definition of L. According to (3.16), L is positive in stable conditions ($q_w < 0$) and is negative in unstable conditions ($q_w > 0$). When appropriately normalised, the mean velocity gradient,

$$\phi_m = \frac{\kappa y}{u_\tau} \frac{\partial u}{\partial y},\tag{3.17}$$

and mean temperature gradient

$$\phi_h = \frac{\kappa u_\tau y}{q_w} \frac{\partial T}{\partial y},\tag{3.18}$$

shall therefore be universal functions of y/L. ϕ_m and ϕ_h are generally approximated by linear expressions y/L (see e.g. Monin et al. 1975),

$$\phi_m\left(\frac{y}{L}\right) = 1 + C_m \frac{y}{L} \quad \text{and} \quad \phi_h\left(\frac{y}{L}\right) = 1 + C_h \frac{y}{L}.$$
 (3.19)

As $y/L \to 0$, i.e. vanishing stratification, the log law (3.3) is recovered from (3.19). In very stable cases, Wyngaard (1973) argued that as a consequence of suppression of vertical motions, the wall distance y cannot enter into the Monin & Obukhov (1954) dimensional analysis. Thus, statistical quantities should become independent of y, e.g. $\phi_m \sim y/L$. Nieuwstadt (1984) and Holtslag & Nieuwstadt (1986) also proposed to extend the validity of the Monin-Obukhov similarity theory beyond the surface layer by considering a local version of L instead, i.e. $\Lambda = T_0 \tau^{3/2}/g\overline{v'T'}$, where τ and $\overline{v'T'}$ are the local turbulent shear stress and turbulent heat flux, respectively, at a certain height y. Observations in the atmosphere (Businger et al. 1971; Kaimal et al. 1976; Nieuwstadt 1984; Metzger & Klewicki 2001) have shown a remarkable agreement with (3.19), both in stable and unstable conditions. Recent numerical simulations at moderate Re have also confirmed the Monin-Obukhov theory for stably stratified flows, both with system rotation (Deusebio et al. 2013a) and without (García-Villalba & del Álamo 2011).

The Monin-Obukhov length scale L also offers an interesting physical interpretation. The wall-bounded turbulent dynamics of stratified flows is a competition between the production of turbulent kinetic energy due to shear

and conversion to potential energy. L provides a measure of the relative importance of these two mechanisms. Assuming that the mean velocity follows the log-law (3.3), the Monin-Obukhov length scale can be interpreted as the distance at which the production,

$$\overline{u'v'}\frac{\partial U}{\partial y} \approx \frac{u_{\tau}^3}{\kappa y},$$
(3.20)

and the turbulent kinetic to potential energy conversion,

$$\frac{g}{T_0}\overline{v'T'} \approx \frac{g}{T_0}q_w,\tag{3.21}$$

are in balance.

At the wall, shear is generally very strong and dominates the dynamics. Even though the temperature/density gradients are sometimes largest at the wall, near-wall structures are little affected by stable stratification (Deusebio et al. 2011) and approximately preserve their spacing of $\approx 100 l^+$, also in strongly stratified continuously turbulent flows. An interesting question is what happens when stratification is so strong that the point y = L approaches the near-wall region. If y = L provides an estimate of the height at which buoyancy becomes of leading order, then as L approaches the near-wall region, the entire boundary layer dynamics becomes buoyancy affected. For very strong stratification, continuously turbulence cannot be sustained, and portions of the flow relaminarise. Figure 3.7 shows the streamwise velocity (defined with respect to the shear stress at the wall) in a horizontal plane close to the wall for an Ekman layer at large stability (Deusebio et al. 2013a). Large portions of the flow undergo relaminarisation which appears in the form of inclined laminar bands. Thus, the flow exhibits strong spatial intermittency. For an even stronger stratification, the inclined patterns further break down into turbulent spots. Similar inclined-bandy structures as the one shown in figure 3.7b have recently been observed in a number of studies of wall-bounded transitional flows, ranging from subcritical low-Re Couette flow (Prigent et al. 2002; Barkley & Tuckerman 2005; Duguet et al. 2010) to stratified open channel flow, rotating Couette flow and magnetohydrodynamic channel flow (Brethouwer et al. 2012). However, the mechanisms underlying their formation and their dynamics are not entirely clear (e.g. for a discussion about their inclination see Duguet & Schlatter 2013).

Several criteria for the onset of relaminarisation in strongly stratified flows have been proposed, adopting non-dimensionless parameters such as the gradient Richardson number (Miles 1961),

$$Ri = \frac{g}{T_0} \frac{\partial T}{\partial y} \left(\frac{\partial u}{\partial y} \right)^{-2} > 0.25, \tag{3.22}$$

the flux Richardson number (Armenio & Sarkar 2002),

$$Ri = \frac{g}{T_0} \frac{\overline{v'T'}}{\overline{u'v'}} \left(\frac{\partial U}{\partial z}\right)^{-1} > 1, \tag{3.23}$$

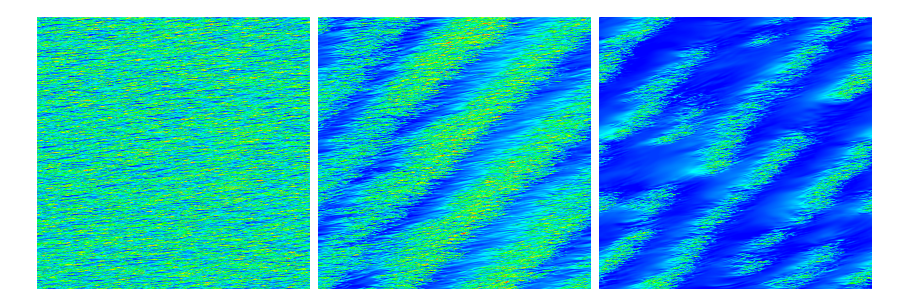


FIGURE 3.7. Instantaneous flow field of the streamwise velocity component u in a wall parallel plane, at $y^+ \approx 12$. From left to right stratification increases as: $L^+ \approx 900$, $L^+ \approx 600$ and $L^+ \approx 250$. Taken from Deusebio et al. (2013a).

or the Nusselt number (García-Villalba & del Álamo 2011),

$$Nu = \frac{q_w h}{\Delta T \kappa_T} \approx 1. (3.24)$$

Here, κ_T is the kinematic diffusivity. More recent studies have proposed criteria based on the Monin-Obukhov length scale, L, rescaled by an outer scale (Nieuwstadt 2005) or the viscous length scale (Flores & Riley 2010). If wall-bounded turbulence is sustained by a near-wall cycle (e.g. Hamilton et al. 1995), inhibition of the near-wall dynamics by buoyancy forces can result in the global relaminarisation of the flow. Thus, it is likely that the criterion should involve near-wall quantities (Flores & Riley 2010). As pointed out by de Wiel et al. (2012), when the flow is driven by external forces, e.g. a pressure gradient, a partial or total relaminarisation is followed by a flow acceleration. As a result of larger shear stresses, turbulence can be triggered again and a global intermittency can arise (García-Villalba & del Álamo 2011).

Ekman boundary layers are of great importance in geophysical flows and understanding how stratification affects their dynamics is crucial for many practical applications. Before the development of computational power, the main source of data was, of course, observations. Even though measurements are able to provide valuable data at very large Re, uncertainties of boundary conditions and unstationarities pose severe limitation to their reliability. Numerical simulations offer a new complementary tool to study stratified Ekman layers. The first numerical simulations of an unstratified turbulent Ekman boundary layers was shortly after followed by its stably (Coleman et al. 1992) and unstably (Coleman et al. 1994) counterparts. Shingai & Kawamura (2002) extended the study of Coleman et al. (1992) by investigating the structure of the Reynolds stresses and the heat fluxes. However, only very limited Re_E , i.e. up to $Re_E = 424$, were considered. More recent numerical investigations have relied on turbulence models in order to increase Re_E (Taylor & Sarkar 2007, 2008b; Zilitinkevich & Esau 2007). However, caution should always be taken when using turbulence models to study strongly stratified flows. LESs significantly

underpredict turbulent transport processes in regions where the stratification is strong and the vertical scales become small (Taylor & Sarkar 2008a). If near-wall dynamics is crucial in the relaminarisation process, transitional flows are also likely to be affected by the use of turbulence models. Therefore, DNSs remain the most accurate and trustworthy tool in the investigation of the stably stratified boundary layer. However, recent progress in the understanding of strongly stratified regime in wall-bounded flows have not considered Ekman boundary layers but have mainly focused to other flow cases (Nieuwstadt 2005; García-Villalba & del Álamo 2011; Brethouwer et al. 2012; Flores & Riley 2010; Deusebio et al. 2011), as channel and open-channel flows. In Paper V, we fill this gap by carrying out a study of the Ekman boundary layer by means of DNSs, ranging from unstratified conditions to very large stability.

CHAPTER 4

Summary of the papers

4.1. Homogeneous turbulence close to geostrophic conditions

We investigate the energy transfer in strongly stratified and rotating systems in order to shed some light on the processes underlying the route to dissipation in geophysical flows. To this end, we carry out numerical simulations of homogeneous turbulence in triply periodic domains forced only at large scales. The high resolutions employed allow us to study more than one dynamical regime within the same simulations.

In paper I, we consider the so-called Primitive Equations, *i.e.* the Boussinesq system in which hydrostatic balance is assumed in the vertical, and we show that two related cascade processes emanate from the same large scale energy source: a downscale cascade of potential enstrophy coexisting with a downscale energy cascade. We find that the amount of energy which is going into the downscale energy cascade decreases monotonically with increased rate of rotation and vanishes in the limit of $Ro \to 0$, reflecting the fact that in quasi-geostrophic turbulence energy is transferred towards large scales. At large scales the dynamics is dominated by a forward enstrophy cascade and energy spectra scale as $\sim k^{-3}$. The forward energy cascade, hidden at large scales, becomes visible only at smaller scales, where it leads to a shallowing of the spectra from $\sim k^{-3}$ to $\sim k^{-5/3}$. This is similar to observations in the atmosphere (Nastrom & Gage 1985), where a transition of kinetic and potential energy spectra from $\sim k^{-3}$ to $\sim k^{-5/3}$ is observed in the mesoscale range, at about 500 kilometres.

In paper II, we extent the study to the full Boussinesq system, thus removing the assumption of hydrostatic balance in the vertical direction. We show that the Primitive Equations can be obtained from the Boussinesq equations by taking the limit $Fr^2/Ro^2 \rightarrow 0$. When Fr^2/Ro^2 is small the difference between the results from the BQ and the PE simulations is found to be small. We find that larger degree of stratification favours a downscale energy cascade, even though the effect of stratification, within the range of parameters representative for large-scale atmospheric dynamics, is weaker as compared to rotation in determining the amount of energy going up- and down-scale. We further investigate the dynamics by considering vertical spectra and we find that Charney isotropy $l_z/l_h \sim f/N$ is approximately valid at larger wave numbers than the the transition wave number. We study the transfer of energy and enstrophy

throughout the turbulent cascade and find that, for intermediate degrees of rotation and stratification, a constant energy flux and a constant enstrophy flux coexist within the same range of scales. In this range, the enstrophy flux is a result of triad interactions involving three geostrophic modes, while the energy flux is a result of triad interactions involving at least one ageostrophic mode, with a dominant contribution from interactions involving two ageostrophic and one geostrophic mode. The role of inertia-gravity waves is studied through analyses of time-frequency spectra of single Fourier modes. Only at large scales, distinct peaks at frequencies predicted for linear waves are observed, whereas at small scales no clear wave activity is observed, suggesting that wave dynamic is negligible within the turbulent cascade. We further analyse the transfer terms and show that resonant-wave triadic interactions cannot explain the downscale energy transfer.

In Paper III, we study the third-order structure functions, focusing at a comparison with measurement in the lower stratosphere. In the range of scales with a downscale energy cascade of kinetic and available potential energy we find that the third order structure functions display a negative linear dependence on separation distance r, in close agreement with the observations in the atmosphere. However, it is also found that terms including the vertical velocity cannot be neglected when the energy flux is estimated. Estimates based on measured structure functions which only include the horizontal velocity component can therefore only provide an order of magnitude estimate of the energy flux. We also calculate the third order velocity structure functions that are not parity invariant and therefore display a cyclonic-anticyclonic asymmetry. In close agreement with the results from the stratosphere we find that these functions have an approximate r^2 -dependence, with strong dominance of cyclonic motions.

In Paper IV, we discuss the effect of vertical confinement in homogeneous rotating turbulence. Vertical confinement is achieved by imposing the vertical periodicity of the flow and by preventing energy to be transferred towards larger vertical scales. Thus, boundary effects arising at solid walls are neglected. In agreement with previous findings, we find that both confinement and rotation favour an inverse energy cascade. However, we show that for moderate rotation rates the direct energy cascade can be recovered by vertically extending the computational box, *i.e.* reducing the lowest vertical wave number which can be represented in the simulation.

4.2. Wall bounded stratified turbulence

As described in paper VII, an existing code, used to study turbulent channel flows, has been largely modified in order to efficiently simulate flows which are bounded by one solid wall only, as for instance the Ekman boundary layer. The Gauss-Lobatto grid in the wall-normal direction, used in conjunction to a spectral discretisation based on Chebyshev polynomials, leads to a clustering of points at the free boundary, which is superfluous in open flows since

turbulence is usually weak or non-existent at the upper boundary. By restricting ourselves to flows with a free-shear surface, we note that equation (3.5) can be viewed as a symmetric conditions for u and w, and a anti-symmetric condition for v at $\tilde{y}=(y-L_y)/L_y=0$. Thus, we modify the numerical algorithm such that, depending on the considered variable, only one parity of the Chebyshev polynomials is retained. Since Gauss-Lobatto grids are coarser at $\tilde{y}=0$, the clustering of points at the free-shear surface is avoided. In order to guarantee the speed-up of the code, an alternative formulation of the Fast Fourier/Chebyshev transforms which accounts for the symmetry is presented. Since we aim at carrying out direct numerical simulations at reasonably high Reynolds numbers, the modifications have been implemented both in a one-dimensional (plane by plane) and two-dimensional (stencil) parallelisation strategy. As an effect of the more efficient discretisation, we show that the number of points in the vertical direction can be reduced, leading to an overall speed-up of the code.

In paper V, we use this code to carry out a series of high-resolution numerical simulations of the turbulent Ekman layer at moderately high Reynolds number, $1600 < Re_E < 3000$. We present results for both neutrally, moderately and strongly stably stratified conditions. For unstratified cases, large-scale structures penetrating from the outer region down to the wall are observed. These structures have a clear dominant frequency and can be related to periodic oscillations or instabilities developing near the low-level jet. We investigate the effect of stratification and Re_E on one-point and two-point statistics, focusing on the turbulent length scales. In the strongly stratified Ekman layer we observe coexisting large-scale laminar and turbulent patches appearing in the form of inclined bands, consistent with other wall-bounded flows. For weaker stratification, continuously sustained turbulence affected by buoyancy is produced. We discuss the scaling of turbulent length scales, the height of the Ekman layer, the friction velocity, the shear angle at the wall and the heat flux. The boundary layer thickness, the friction velocity and the shear angle are shown to depend on Lf/u_{τ} , whereas the heat fluxes shows a better scaling when plotted versus $L^+ = Lu_\tau/\nu$.

The helicity dynamics in neutrally stratified Ekman boundary layers is investigated in Paper VI. We define cyclonic and anticyclonic helicity with respect to the sign of $\Omega \cdot e_y \mathcal{H}$, where Ω is the rotation vector and e_y is the wall normal unit vector, positive for cyclonic helicity and negative for anticyclonic helicity. We find that there is a preference for cyclonic helicity in the lower part of the Ekman layer and anticyclonic helicity in the uppermost part. We derive the evolution equations for the mean field helicity and the mean turbulent helicity and show that the pressure term injects cyclonic helicity at a rate $2\Omega G^2$ over the total depth of the Ekman layer, where G is the geostrophic wind far from the wall. A substantial part of the mean field helicity is transferred to turbulent helicity which is ultimately destroyed by viscous effects. The helicity spectrum

40 4. SUMMARY OF THE PAPERS

displays a dependence close to $\sim k^{-5/3}$ in an intermediate range of scales. Although the limited extent of this range prevents an accurate comparison with theoretical predictions, results suggest the existence of a forward helicity cascade in the log-layer of Ekman boundary layers, as the one occurring in the atmosphere and oceans.

CHAPTER 5

Conclusions and outlook

Since their maturity, digital computers have allowed for a number of advances in the understanding of turbulent processes. Their use have greatly increased over the years and is expected to increase even further in the future. In this thesis, it has been shown how numerical simulations can be used to study wall-bounded and homogeneous turbulence affected by stratification and rotation, allowing for some insights into the atmospheric and oceanic turbulent dynamics.

5.1. Turbulence close to geostrophy: A key for improving weather forecast...

We have analysed the dynamics in strongly stratified and rotating turbulence by means of box simulations of homogeneous turbulence, ranging from the QG limit to small but finite rotation rates and degrees of stratification. The use of an idealised setup made it possible to study the backbone mechanism for the energy transfer underlying rotating and stratified turbulence dynamics, free of the additional complexities present in measurements and global atmospheric models, such as topography, cloud dynamics, etc. Numerical simulations, although sometimes non-physical, allow to arbitrarily remove or separate the different contributions and to identify the key factors controlling the dynamics.

Unlike QG turbulence, where almost all turbulent energy cascades upscale, finite rotation rates lead to a leakage of energy towards small scales and, as a consequence, a forward energy cascade. This process can explain the existence of a $\sim k^{-5/3}$ range in the atmosphere, interpreted as a downscale energy cascade range, and solve the apparent paradox of how and where dissipation can take place in flows close to geostrophic conditions. Even though motions which are not in geostrophic balance are, at large scales, small compared to the geostrophic motions, they have a crucial role in transferring the energy downscale. Great care should thus be taken in representing such motions in atmospheric models.

Despite the idealised setup, energy spectra and structure functions show remarkable agreement with measurements in the atmosphere, suggesting that the scenario of a hidden cascade emanating from the largest scales can explain the observations. Recent analyses of data of global circulating models (GCMs) also show strong similarities with these findings (Augier & Lindborg 2013). One open question is whether such a process may occur also in the oceans. Indeed, observations are more difficult and there is great uncertainty regarding

the kinetic energy budget (Ferrari & Wunsch 2009). Nevertheless, baroclinic instabilities have a key-role in oceanic dynamics as well and a double cascade of energy originates at the deformation radius (Scott & Wang 2005). Moreover, spectra found in the oceans are consistent with the hypothesis of stratified turbulence (Riley & Lindborg 2008). Thus, the dynamical process described in this thesis may also be important in oceanic dynamics.

Numerical simulations can also provide a tool to investigate the energy transfer in rotating turbulent flows. Our results suggest that rotating turbulent flows are not incompatible with the presence of a forward energy cascade. The small-scale dissipations was always observed to monotonically increase with the aspect ratio. Thus, in order to reproduce the forward energy cascade dynamics, computational boxes with large vertical extent may be required. Although our analysis has mainly focused on moderate rotation rates, saturation of the small-scale dissipation has never been observed, even when the rotation rate was large. It is of interest to test whether the direct energy cascade would fully recover also at small Ro. This may, however, require very tall boxes and can be computationally very expensive.

The understanding of how energy is transferred in geophysical flows is of primary importance, not only from a fundamental perspective. Existing atmospheric (and oceanic) models can be evaluated against theoretical predictions, allowing for an assessment of their actual capabilities and deficiencies. Perhaps even more importantly, an understanding of the dynamics governing geophysical flows can provide useful hints and tools to improve the existing models.

Computational power is nowadays at a level that allows us to represent more than one dynamical regime within the same simulation. In the present study, the transition between a strongly-rotating strongly-stratified regime to a strongly stratified regime has been the main focus. There are indeed other transitional dynamics of practical interests, as, for instance, the transition between strongly stratified dynamics and three-dimensional turbulence. The latter involves the non-trivial interplay of different length scale involved in the dynamics, as the buoyancy scale l_b and the Ozmidoz length scale l_O (Augier et al. 2012).

Further studies using simple setups may also allow us to shed some light on other issues of practical interest, as, for instance, how predictability changes in highly rotating and stratified turbulent flows. Observations, which are then used as input of GCMs, always suffer from a limited degree of accuracy. Understanding how fast an initial error spreads and contaminates the entire flow is crucial in order to assess the actual reliability of models. Which type of dynamics mainly affects the error propagation can also provide useful guidelines for improving numerical predictions.

5.2. Wall-bounded turbulence and atmospheric boundary layers

We have carried out a series of direct numerical simulations of the Ekman boundary layer, considering neutrally and stably stratified conditions. Thanks to the advancement in computational power, moderately high Reynolds number could be simulated in computational boxes larger than what has been used in previous studies. For neutrally stratified conditions, our results show the presence of large-scale turbulent structure which has not been observed before, possibly prevented by the use of limited computational domains. It is not clear whether such large-scale structures are of similar nature as the large-scale structures observed in other wall-bounded flows. Our results show that they exhibit a strong degree of coherency in the vertical direction and that their signatures can be found close to the wall, therefore suggesting a significant influence on the near-wall dynamics. The strong vertical coherency might also indicate that their origin is connected to a global instability of the flow. Ongoing work is aimed at studying the stability of the turbulent Ekman boundary layers in order to verify such a conjecture.

Stable stratification was introduced in the flows by imposing a temperature difference in the vertical direction and its effect on the wall-bounded turbulent dynamics was investigated. For moderate degrees of stratification, statistically steady continuously turbulent states are observed. The height of the boundary layer drastically reduces and it was shown to agree with theoretical predictions. Despite the limited Re, statistical quantities also showed reasonable agreement with the Monin-Obukhov similarity theory in an intermediate range of scales.

On the other hand, when stratification is very strong the flow partially relaminarises and laminar and turbulent motions coexist, similar to what is found in other studies of transitional flows. The dynamics of laminar/turbulent patterns is, at current state, not fully understood and further studies should be aimed to better describe this regime. One open question concerns the condition for the appearance of laminar regions. In strongly stratified flows, our simulations show laminar patches already at $L^+\approx 500$, thus larger than the criterion suggested by Flores & Riley (2010) for open-channel flows, i.e. $L^+\approx 100$. However, since only one moderately high Re was considered in the study, it is not possible to assess whether the L^+ criterion is appropriate and what should be the actual value at which laminar regions appear. Although computationally expensive, reliable studies of the relaminarisation process should always consider boxes large enough to fit the presence of both laminar and turbulent patches, as in the current study.

The database produced by numerical simulations gives a full knowledge of the flow, which can be very valuable. In the present context, it has been used to study the helicily dynamics in atmospheric boundary layers (Deusebio & Lindborg 2013). It has been found that the Ekman boundary layer is highly helical and that a downscale helicity turbulent cascade exists within the logarithmic region. This remarkable result suggest that signatures of the breaking

44 5. CONCLUSIONS AND OUTLOOK

of parity invariance observed in large-scale geophysical flows are transferred downscale to the smallest scale of motions of the flow, *i.e.* to the Kolmogorov scale. This new finding also opens the possibility of testing theories on the helicity cascade at very large Reynolds numbers by means of measurements in an atmospheric boundary layer, where Re is typically of the order of 10^6 , unfeasible in numerical simulations.

Acknowledgments

This work is not only a doctoral thesis, but it is also - in my personal perspective - the logbook of a journey, of an adventure which has filled my life in the last four years. And, as any other journey, it would not have been possible without the help of all the people I met along the way. Each one has, in a way or another, contributed to it. Without you, this work (and this journey) would not have been the same. *Grazie!*

In primis - my gratitude goes to my supervisor captain Erik Lindborg not only for being my guide in this journey but, most of all, for trasmitting and sharing his tremendous passion for science and his romantic view of research. It has been an honour and a pleasure to be side by side in these years, which I will never forget. Tack så mycket! Every journey has a beginning. Mine started with an e-mail from Philipp Schlatter who I would like to personally thank for both attracting me in Stockholm and for sharing, over the years, his knowledge on numerics and simulations. I would like to thank Geert Brethouwer for all the fruitful discussions we had and for supporting me in my very first conference in Rome. I wish to kindly thank Guido Boffetta, for hosting me in Turin and for the very many interesting discussions, not only on scientific matters. A special thank goes to Anders Dahlkild who has kindly read and provided comments on this "logbook".

Any success is not worth being lived if there is no one to share the happiness with. And when some bad moments come, being a difficulty in the Phd or a broken elbow, it is important to have people that make you feel you are not alone. Andreas Vallgren and Pierre Augier, thanks for being great workmates and good friends at the same time. Thank you Amin for being such a great room-mate over all these years. I wish you, Zeinab and Rayan-Zackaria all the best on your new adventure, all together. A huge thank also goes to all those people I had the luck to share my everyday life with: Nima, Daniel, Onofrio, Nicolo, Qiang, Gabriele, Zeinab, George, Ardheshir, Lailai, Armin, Joy, Taras, Werner, Iman, Francesco, Luca Brandt, Luca Biancofiore, Gaetano, Ruth, Azad, Cai-Juan, Igor, Peter, Marit, Krishna, Bernhard, Mihai, Timea, Walter, Reza, Ellinor, Karl, Christina and Heide. Ett särskilt tack till Bubba för din hjälp och ditt oändliga tålamod med min svenska. Tristan, Valentina, Karin,

Marta, Emmelie, Michele, Alessandro and Serena, thanks for the unforgettable time here in Stockholm and for cheering me up in many many occasions. I would also like to thank Angela, Nic, Jean-An, Alex, Berghem and Lu, for being, despite the distance, always good friends I can count on.

But, in any journey, the most important thing is to never get lost. I wish to dedicate this work to my cardinal points, to those stars that by shining bright in the sky always indicate the right direction.

Sara, thanks for always supporting me and believing in me, beyond any possible human limit.

Mamma e Papá, grazie per esserci, sempre e comunque, per avere sempre tempo per ascoltare e per, nonostante i 2000 chilometri, farmi sempre sentire a casa.

La *mezza* é stata uno dei giorni piú belli qui a Stoccolma, grazie a *Lorenzo* per essere stato parte di quel giorno e di mille altri ricordi che, sopratutto nei momenti di difficoltà, danno la forza ad andare avanti.

Un grazie particolare va infine a colei che ha ispirato ogni passo di questo cammino, perché, di ogni passo, era la direzione. Grazie per essere stata, di questo viaggio, la musa e la meta. *Ti amo, Dada!*

Bibliography

- Andreas, E. L., Claffey, K. J., Jordan, R. E., Fairall, C. W., Guest, P. S., Persson, P. O. G. & Grachev, A. A. 2006 Evaluations of the von Kármán constant in the atmospheric surface layer. *J. Fluid Mech.* **559**, 117–150.
- Antonia, R. A., Ould-Rouis, M., Anselmet, F. & Zhu, Y. 1997 Analogy between predictions of kolmogorov and yaglom. *J. Fluid Mech.* **332** (1), 395–409.
- Armenio, V. & Sarkar, S. 2002 An investigation of stably stratified turbulent channel flow using large-eddy simulation. *J. Fluid Mech.* **459**, 1–42.
- Augier, P., Billant, P. & Chomaz, J. M. 2013 Stratified turbulence forced with columnar dipoles. Numerical study. *Submitted to J. Fluid Mech.*
- Augier, P., Chomaz, J. M. & Billant, P. 2012 Spectral analysis of the transition to turbulence from a dipole in stratified fluid. *J. Fluid Mech.* **713**, 86–108.
- Augier, P. & Lindborg, E. 2013 A new formulation of the spectral energy budget of the atmosphere, with application to two high-resolution general circulation models. *J. Atmos. Sci.* **70** (70), 2293–2308.
- Banta, R. M., Mahrt, L., Vickers, D., Sun, J., Balsley, B. B., Pichugina, Y. L. & Williams, E. J. 2007 The very stable boundary layer on nights with weak low-level jets. *J. Atmos. Sci.* **64** (9), 3068–3090.
- Barkley, D. & Tuckerman, L. S. 2005 Computational study of turbulent laminar patterns in Couette flow. *Phys. Rev. Lett.* **94** (1), 014502.
- Bartello, P., Metais, O. & Lesieur, M. 1994 Coherent structures in rotating three-dimensional turbulence. *J. Fluid Mech.* 273, 1–30.
- Bellet, F., Godeferd, F. S., Scott, J. F. & Cambon, C. 2006 Wave turbulence in rapidly rotating flows. *J. Fluid Mech.* **562** (1), 83–121.
- Benzi, R., Biferale, L. & Parisi, G. 1993 On intermittency in a cascade model for turbulence. *Physica D: Nonlinear Phenomena* **65** (1-2), 163–171.
- BIFERALE, L., MUSACCHIO, S. & TOSCHI, F. 2012 Inverse energy cascade in three-dimensional isotropic turbulence. *Phys. Rev. Lett.* **108** (16), 164501.
- BIFERALE, L. & TOSCHI, F. 2001 Anisotropic homogeneous turbulence: Hierarchy and intermittency of scaling exponents in the anisotropic sectors. *Phys. Rev. Lett.* **86**, 4831–4834.
- BILLANT, P. & CHOMAZ, J.-M. 2000 Experimental evidence for a new instability of a vertical columnar vortex pair in a strongly stratified fluid. *J. Fluid Mech.* 418, 167–188.

- BILLANT, P. & CHOMAZ, J.-M. 2001 Self-similarity of strongly stratified inviscid flows. *Phys. Fluids* **13** (6), 1645–1651.
- BOFFETTA, G. 2007 Energy and enstrophy fluxes in the double cascade of two-dimensional turbulence. J. Fluid Mech. 589, 253–260.
- BOUSSINESQ, J. 1877 Essai sur la the'orie des eaux courantes. *Imprimerie nationale J. sav. 1'Acad. des Sci.* .
- Brethouwer, G., Billant, P., Lindborg, E. & Chomaz, J.-M. 2007 Scaling analysis and simulation of strongly stratified turbulent flows. *J. Fluid Mech.* **585**, 343–368.
- Brethouwer, G., Duguet, Y. & Schlatter, P. 2012 Turbulent–laminar coexistence in wall flows with Coriolis, buoyancy or Lorentz forces. *J. Fluid Mech.* 704, 137.
- BRISSAUDW, A., FRISCH, U., LEORAT, J., LESIEUR, M. & MAZURE, A. 1973 Helicity cascades in fully developed isotropic turbulence. *Phys. Fluids* **16**, 1366.
- Buckingham, E. 1914 On physically similar systems; illustrations of the use of dimensional equations. *Phys. Rev.* 4 (4), 345–376.
- Businger, J., Wyngaard, J. C., Izumi, Y. & Bradley, E. F. 1971 Flux-profile relationships in the atmospheric surface layer. *J. Atmos. Sci.* 28 (2), 181–189.
- CALDWELL, D. R. & ATTA, C. W. V. 1970 Characteristics of Ekman boundary layer instabilities. J. Fluid Mech. 44 (1), 79–95.
- Cambon, C., Mansour, N. N. & Godeferd, F. S. 1997 Energy transfer in rotating turbulence. *J. Fluid Mech.* 337, 303–332.
- CANUTO, C., HUSSAINI, M. Y., QUARTERONI, A. & ZANG, T. A. 1988 Spectral methods in Fluid Dynamics. Springer-Verlag.
- Celani, A., Musacchio, S. & Vincenzi, D. 2010 Turbulence in more than two and less than three dimensions. *Phys. Rev. Lett.* **104** (18), 184506.
- Charney, J. G. 1971 Geostrophic turbulence. J. Atmos. Sci. 28 (6), 1087–1094.
- Chen, Q., Chen, S., Eyink, G. L. & Holm, D. D. 2003 Intermittency in the joint cascade of energy and helicity. *Phys. Rev. Lett.* **90** (21), 214503.
- CHEN, Q., CHEN, S., EYINK, G. L. & HOLM, D. D. 2005 Resonant interactions in rotating homogeneous three-dimensional turbulence. J. Fluid Mech. 542, 139– 164.
- Cho, J. Y. N. & Lindborg, E. 2001 Horizontal velocity structure functions in the upper troposphere and lower stratosphere: 1. observations. *J. Geophys. Res.* **106** (D10), 10223–10232.
- COLEMAN, G. N., FERZIGER, J. H. & SPALART, P. R. 1990 A numerical study of the turbulent Ekman layer. *J. Fluid Mech.* **213**, 313–348.
- COLEMAN, G. N., FERZIGER, J. H. & SPALART, P. R. 1992 Direct simulation of the stably stratified turbulent Ekman layer. *J. Fluid Mech.* **244** (1), 677–712.
- Coleman, G. N., Ferziger, J. H. & Spalart, P. R. 1994 A numerical study of the convective boundary layer. *Boun.-Lay. Meteorol.* **70** (3), 247–272.
- DAVIDSON, P. A., KANEDA, Y. & SREENIVASAN, K. R. 2012 Ten Chapters in Turbulence. Cambridge University Press.
- Davidson, P. A., Staplehurst, P. J. & Dalziel, S. B. 2006 On the evolution of eddies in a rapidly rotating system. *J. Fluid Mech.* **557** (1), 135–144.
- Deardorff, J. W. 1970 A numerical study of three-dimensional turbulent channel flow at large Reynolds numbers. *J. Fluid Mech.* 41, 453–480.

- DEL ÁLAMO, J. C., JIMÉNEZ, J., ZANDONADE, P. & MOSER, R. D. 2006 Self-similar vortex clusters in the turbulent logarithmic region. *J. Fluid Mech.* **561**, 329–358.
- DERBYSHIRE, S. H. 1999 Boundary-layer decoupling over cold surfaces as a physical boundary-instability. *Boun.-Lay. Meteorol.* **90** (2), 297–325.
- Deusebio, E., Brethouwer, G., Schlatter, P. & Lindborg, E. 2013a A numerical study of the unstratified and stratified Ekman layer. Submitted to J. Fluid Mech.
- DEUSEBIO, E. & LINDBORG, E. 2013 Helicity in the Ekman boundary layer. Submitted to J. Fluid Mech.
- Deusebio, E., Schlatter, P., Brethouwer, G. & Lindborg, E. 2011 Direct numerical simulations of stratified open channel flows. *J. Phys.: Conf. Ser.* **318** (2), 022009.
- DEUSEBIO, E., VALLGREN, A. & LINDBORG, E. 2013b The route to dissipation in strongly stratified and rotating flows. J. Fluid Mech. 720, 66–103.
- Domaradzki, J. A. & Saiki, E. M. 1997 A subgrid-scale model based on the estimation of unresolved scales of turbulence. *Phys. Fluids* **9** (7), 2148–2164.
- Duguet, Y. & Schlatter, P. 2013 Oblique laminar-turbulent interfaces in plane shear flows. *Phys. Rev. Lett.* **110** (3), 034502.
- Duguet, Y., Schlatter, P. & Henningson, D. S. 2010 Formation of turbulent patterns near the onset of transition in plane Couette flow. *J. Fluid Mech.* **650**, 119.
- EKMAN, V. W. 1905 On the influence of the Earth's rotation on ocean currents. *Arch. Math. Astron. Phys.* 2, 1–52.
- Embid, P. F. & Majda, A. J. 1998 Low Froude number limiting dynamics for stably stratified flow with small or finite Rossby numbers. *Geophys. Astro. Fluid Dyn.* 87 (1-2), 1–50.
- ETLING, D. & Brown, R. A. 1993 Roll vortices in the planetary boundary layer: A review. *Boun.-Lay. Meteorol.* **65** (3), 215–248.
- FALLER, A. J. 1963 An experimental study of the instability of the laminar Ekman boundary layer. *J. Fluid Mech.* **15** (163), 560–576.
- Faller, A. J. & Kaylor, R. E. 1966 A numerical study of the instability of the laminar Ekman boundary layer. *J. Atmos. Sci.* **23**, 466–480.
- Ferrari, R. & Wunsch, C. 2009 Ocean Circulation Kinetic Energy: Reservoirs, Sources, and Sinks. *Ann. Rev. Fluid Mech.* 41, 253–282.
- Feynman, R. P. 1964 Feynman lectures on physics. Addison-Wesley.
- Flores, O. & Riley, J. J. 2010 Analysis of turbulence collapse in stably stratified surface layers using direct numerical simulation. *Boun.-Lay. Meteorol.* **129** (2), 241–259.
- Frehlich, R., Meillier, Y. & Jensen, M. L. 2008 Measurements of boundary layer profiles with in situ sensors and doppler lidar. *J. Atmos. Oceanic Tech.* **25**, 1328
- Frisch, U. 1996 Turbulence. Cambridge University Press.
- GARCÍA-VILLALBA, M. & DEL ÁLAMO, J. C. 2011 Turbulence modification by stable stratification in channel flow. *Phys. Fluids* **23** (4), 045104.
- GARGETT, A. E., HENDRICKS, P. J., SANFORD, T. B., OSBORN, T. R. & WILLIAMS, A. J. 1981 A composite spectrum of vertical shear in the upper ocean. J. Phys. Oceanogr. 11, 1258–1271.

- GATSKI, T. B. & SPEZIALE, C. G. 1993 On explicit algebraic stress models for complex turbulent flows. *J. Fluid Mech.* **254**, 59–78.
- Gence, J. N. & Frick, C. 2001 Naissance des corrélations triples de vorticité dans une turbulence statistiquement homogène soumise à une rotation. *Comptes Rendus de l'Académie des Sciences-Series IIB-Mechanics* **329** (5), 351–356.
- GERMANO, M. 1992 Turbulence The filtering approach. J. Fluid Mech. 238, 325–336.
- GERMANO, M., PIOMELLI, U., MOIN, P. & CABOT, W. H. 1991 A dynamic subgrid-scale eddy viscosity model. *Phys. Fluids* 3 (7), 1760–1765.
- GILL, A. E. 1982 Atmosphere-ocean dynamics. Academic Press, New York.
- Grant, H. L., Stewart, R. W. & Moilliet, A. 1962 Turbulence spectra from a tidal channel. *J. Fluid Mech.* 12 (2), 241–268.
- Griffa, A., Lumpkin, R. & Veneziani, M. 2008 Cyclonic and anticyclonic motion in the upper ocean. *Geophys. Res. Lett.* **35** (1), L01608.
- Hamilton, J. H., Kim, J. & Waleffe, F. 1995 Regeneration mechanisms of nearwall turbulence structures. *J. Fluid Mech.* **287**, 317–348.
- HAMILTON, K., TAKAHASHI, Y. O. & OHFUCHI, W. 2008 Mesoscale spectrum of atmospheric motions investigated in a very fine resolution global general circulation model. J. Geophys. Res. 113 (18).
- VAN HEIJST, G. J. F. & KLOOSTERZIEL, R. C. 1989 Tripolar vortices in a rotating fluid pp. 569–571.
- HOLTSLAG, A. A. M. & NIEUWSTADT, F. T. M. 1986 Scaling the atmospheric boundary layer. *Boun.-Lay. Meteorol.* **36** (1-2), 201–209.
- HOPFINGER, E. J., BROWAND, F. K. & GAGNE, Y. 1982 Turbulence and waves in a rotating tank. *J. Fluid Mech.* **125**, 505–534.
- HOPFINGER, E. J. & VAN HEIJST, G. J. F. 1993 Vortices in rotating fluids. *Ann. Rev. Fluid Mech.* **25** (1), 241–289.
- HOYAS, S. & JIMÉNEZ, J. 2006 Scaling of the velocity fluctuations in turbulent channels up to $Re_{\tau}=2003$. Phys. Fluids **18** (1), 011702.
- HULTMARK, M., VALLIKIVI, M., BAILEY, S. C. C. & SMITS, A. J. 2012 Turbulent pipe flow at extreme Reynolds numbers. *Phys. Rev. Lett.* **108** (9), 094501.
- IBBETSON, A. & TRITTON, D. J. 1975 Experiments on turbulence in a rotating fluid. J. Fluid Mech. 68 (04), 639–672.
- JIMÉNEZ, J. 2012 Cascades in wall-bounded turbulence. Ann. Rev. Fluid Mech. 44, 27–45.
- KAIMAL, J. C., WYNGAARD, J. C., HAUGEN, D. A., COTÉ, O. R., IZUMI, Y., CAUGHEY, S. J. & READINGS, C. J. 1976 Turbulence structure in the convective boundary layer. *J. Atmos. Sci.* **33** (11), 2152–2169.
- Kaneda, Y., Ishihara, T., Yokokawa, M., Itakura, K. & Uno, A. 2003 Energy dissipation rate and energy spectrum in high resolution direct numerical simulations of turbulence in a periodic box. *Phys. Fluids* **15** (2), L21–L24.
- KIM, J., MOIN, P. & MOSER, R. 1987 Turbulence statistics in fully developed channel flow at low Reynolds number. J. Fluid Mech. 177, 133–166.
- KITAMURA, Y. & MATSUDA, Y. 2006 The k_H^{-3} and $k_H^{-5/3}$ energy spectra in stratified turbulence. *Geophys. Res. Lett.* **33**, L05809.
- Kloosterziel, R. C. & van Heijst, G. J. F. 1991 An experimental study of unstable barotropic vortices in a rotating fluid. *J. Fluid Mech* **223** (1).

- Kolmogorov, A. N. 1941a Dissipation of energy in locally isotropic turbulence [In Russian]. *Dokl. Akad. Nauk SSSR* **32**, 19–21.
- Kolmogorov, A. N. 1941b The local structure of turbulence in incompressible viscous fluid for very large Reynolds numbers [In Russian]. *Dokl. Akad. Nauk SSSR* **30.** 299–303.
- KONDO, J., KANECHIKA, O. & YASUDA, N. 1978 Heat and momentum transfers under strong stability in the atmospheric surface layer. *J. Atmos. Sci.* **35** (6), 1012–1021.
- Kraichnan, R. H. 1967 Inertial ranges in two-dimensional turbulence. *Phys. Fluids* **10** (7), 1417–1423.
- Legras, B., Santangelo, P. & Benzi, R. 1988 High-resolution numerical experiments for forced two-dimensional turbulence. *Europhys. Lett.* 5, 37.
- LEMONE, M. A. 1973 The structure and dynamics of horizontal roll vortices in the planetary boundary layer. J. Atmos. Sci. 30 (6), 1077–1091.
- LILLY, D. K. 1966 On the instability of Ekman boundary flow. J. Atmos. Sci. 23 (5), 481–494.
- LILLY, D. K. 1983 Stratified turbulence and the mesoscale variability of the atmosphere. J. Atmos. Sci. 40 (3), 749–761.
- LILLY, D. K. 1986 The structure, energetics and propagation of rotating convective storms. Part II: Helicity and storm stabilization. J. Atmos. Sci. 43 (2), 126–140.
- LINDBORG, E. 1999 Can the atmospheric kinetic energy spectrum be explained by two-dimensional turbulence? *J. Fluid Mech.* **388**, 259–288.
- LINDBORG, E. 2006 The energy cascade in a strongly stratified fluid. J. Fluid Mech. ${\bf 550},\,207-242.$
- LINDBORG, E. & BRETHOUWER, G. 2007 Stratified turbulence forced in rotational and divergent modes. J. Fluid Mech. 586, 83–108.
- LINDBORG, E. & CHO, J. Y. N. 2000 Determining the cascade of passive scalar variance in the lower stratosphere. *Phys. Rev. Lett.* **85** (26), 5663.
- LINDBORG, E. & Cho, J. Y. N. 2001 Horizontal velocity structure functions in the upper troposphere and lower stratosphere: 2. theoretical considerations. *Journal of Geophysical Research: Atmospheres* (1984–2012) **106** (D10), 10233–10241.
- LORENZ, E. N. 1963 Deterministic nonperiodic flow. J. Atmos. Sci. 20, 130–148.
- Mahrt, L. 1998 Nocturnal boundary-layer regimes. *Boun.-Lay. Meteorol.* **88** (2), 255–278.
- Maltrud, M. E. & Vallis, G. K. 1993 Energy and enstrophy transfer in numerical simulations of two-dimensional turbulence. *Phys. Fluids* 5, 1760–1775.
- Marusic, I. & Kunkel, G. J. 2003 Streamwise turbulence intensity formulation for flat-plate boundary layers. *Phys. Fluids* **15**, 2461.
- Marusic, I., McKeon, B. J., Monkewitz, P. A., Nagib, H. M., Smits, A. J. & Sreenivasan, K. R. 2010 Wall-bounded turbulent flows at high Reynolds numbers: Recent advances and key issues. *Phys. Fluids* **22**, 065103.
- Marusic, I., Monty, J. P., Hultmark, M. & Smits, A. J. 2013 On the logarithmic region in wall turbulence. *J. Fluid Mech.* **716**, R3.
- MATHIS, R., MARUSIC, I., HUTCHINS, N. & SREENIVASAN, K. R. 2011 The relationship between the velocity skewness and the amplitude modulation of the small scale by the large scale in turbulent boundary layers. *Phys. Fluids* **23** (12), 121702–121702.

- METZGER, M. M. & KLEWICKI, J. C. 2001 A comparative study of near-wall turbulence in high and low Reynolds number boundary layers. *Phys. Fluids* **13**, 692.
- MILES, J. W. 1961 On the stability of heterogeneous shear flows. *J. Fluid Mech.* **10** (4), 496–508.
- MILLIKAN, C. B. 1938 A critical discussion of turbulent flows in channels and circular tubes. In *Proc. 5th Int. Congr. Appl. Mech*, pp. 386–392.
- MININNI, P. D. & POUQUET, A. 2009 Helicity cascades in rotating turbulence. *Phys. Rev. E* **79** (2), 026304.
- MOFFATT, H. K. 1969 The degree of knottedness of tangled vortex lines. *J. Fluid Mech.* **35** (1), 117–129.
- Moin, P. & Mahesh, K. 1998 Direct numerical simulation: a tool in turbulence research. *Ann. Rev. Fluid Mech.* **30** (1), 539–578.
- Moisy, F., Morize, C., Rabaud, M. & Sommeria, J. 2011 Decay laws, anisotropy and cyclone–anticyclone asymmetry in decaying rotating turbulence. *J. Fluid Mech.* **666**, 5–35.
- MONIN, A. A. S., YAGLOM, A. M. & LUMLEY, J. L. 1975 Statistical Fluid Mechanics: Mechanics of Turbulence, , vol. 2. MIT Press.
- Monin, A. S. & Obukhov, A. M. 1954 Basic laws of turbulent mixing in the surface layer of the atmosphere. *Contrib. Geophys. Inst. Acad. Sci. USSR* **151**, 163–187.
- Monkewitz, P. A., Chauhan, K. A. & Nagib, H. M. 2007 Self-consistent high-Reynolds-number asymptotics for zero-pressure-gradient turbulent boundary layers. *Phys. Fluids* **19**, 115101.
- MORIZE, C. & MOISY, F. 2006 Energy decay of rotating turbulence with confinement effects. *Phys. Fluids* **18** (6), 065107–065107.
- Moser, R. D. & Moin, P. 1987 The effects of curvature in wall-bounded turbulent flows. J. Fluid Mech. 175, 479-510.
- NANSEN, F. 1905 The Norwegian North polar expedition, 1893-1896: Scientific results. Longmans, Green and Company.
- NASTROM, G. D. & GAGE, K. S. 1985 A climatology of atmospheric wavenumber spectra of wind and temperature observed by commercial aircraft. *J. Atmos. Sci.* 42, 950–960.
- NASTROM, G. D., GAGE, K. S. & JASPERSON, W. H. 1984 Kinetic energy spectrum of large-and mesoscale atmospheric processes. *Nature* **310** (5972), 36–38.
- Nieuwstadt, F. T. M. 1984 The turbulent structure of the stable, nocturnal boundary layer. J. Atmos. Sci. 41 (14), 2202–2216.
- NIEUWSTADT, F. T. M. 2005 Direct numerical simulation of stable channel flow at large stability. *Boun.-Lay. Meteorol.* **116**, 277–299.
- Obukhov, A. M. 1946 Turbulence in the atmosphere with inhomogeneous temperature. Trudy geofiz. inst. AN SSSR ${f 1}$.
- Ohkitani, K. 1990 Nonlocality in a forced two-dimensional turbulence. *Phys. Fluids* **2** (9), 1529–1531.
- Ohkitani, K. & Kida, S. 1992 Triad interactions in a forced turbulence. *Phys. Fluids* 4 (4), 794–802.
- Orszag, S. A. & Patterson, G. S. 1972 Numerical simulation of three-dimensional homogeneous isotropic turbulence. *Phys. Rev. Lett.* 28, 76–79.

- ÖSTERLUND, J. M., JOHANSSON, A. V., NAGIB, H. M. & HITES, M. H. 2000 A note on the overlap region in turbulent boundary layers. *Phys. Fluids* **12** (1), 1.
- OZMIDOV, R. V. 1965 On the turbulent exchange in a stably stratified ocean. *Izv. Acad. Sci. USSR*, *Atmos. Oceanic Phys.* 1, 493–497.
- Pedlosky, J. 1987 Geophysical Fluid Dynamics. Springer.
- Pope, S. B. 2000 Turbulent flows. Cambridge university press.
- Prigent, A., Grégoire, G., Chaté, H., Dauchot, O. & van Saarloos, W. 2002 Large-scale finite-wavelength modulation within turbulent shear flows. *Phys. Rev. Lett.* **89** (1), 6465.
- PROUDMAN, J. 1916 On the motion of solids in a liquid possessing vorticity. *Proc. Roy. Soc. London* **92** (642), 408–424.
- RASAM, A., BRETHOUWER, G., SCHLATTER, P., LI, Q. & JOHANSSON, A. V. 2011 Effects of modelling, resolution and anisotropy of subgrid-scales on large eddy simulations of channel flow. *J. Turb.* p. N10.
- REYNOLDS, O. 1886 On the theory of lubrication and its application to Mr. Beauchamp Tower's experiments, including an experimental determination of the viscosity of olive oil. *Philos. Trans. R. Soc. Lond.*, *I* **177**, 157–234.
- REYNOLDS, O. 1895 On the dynamical theory of incompressible viscous fluids and the determination of the criterion. *Philos. Trans. R. Soc. Lond.*, A 186, 123–164.
- REYNOLDS, W. C. 1990 The potential and limitations of direct and large eddy simulations. In *Whither Turbulence? Turbulence at the Crossroads*, , vol. 357, pp. 313–343.
- RICHARDSON, L. F. 1922 Weather Prediction by Numerical Process. Dover Publications, Inc., New York.
- RILEY, J. J. & DEBRUYNKOPS, S. M. 2003 Dynamics of turbulence strongly influenced by buoyancy. *Phys. Fluids* **15** (7), 2047–2059.
- RILEY, J. J. & LINDBORG, E. 2008 Stratified turbulence: A possible interpretation of some geophysical turbulence measurements. J. Atmos. Sci. 65 (7), 2416–2424.
- RILEY, J. J., METCALFE, R. W. & WEISSMAN, M. A. 1981 Direct numerical simulations of homogeneous turbulence in density-stratified fluids. *AIP Conf. Proceed.* **76** (1), 79–112.
- ROSENBERG, B. J., HULTMARK, M., VALLIKIVI, M., BAILEY, S. C. C. & SMITS, A. J. 2013 Turbulence spectra in smooth-and rough-wall pipe flow at extreme reynolds numbers. *J. Fluid Mech.* **731**, 46–63.
- Schlatter, P. & Örlü, R. 2010 Assessment of direct numerical simulation data of turbulent boundary layers. *J. Fluid Mech.* **659** (1), 116–126.
- Schlatter, P., Örlü, R., Li, Q., Brethouwer, G., Fransson, J. H. M., Johansson, A. V., Alfredsson, P. H. & Henningson, D. S. 2009 Turbulent boundary layers up to $Re_{\theta}=2500$ studied through simulation and experiment. *Phys. Fluids* **21** (5), 051702.
- Scott, R. B. & Wang, F. 2005 Direct evidence of an oceanic inverse kinetic energy cascade from satellite altimetry. *J. Phys. Oceanogr.* **35** (9), 1650–1666.
- Scott, R. K. 2007 Nonrobustness of the two-dimensional turbulent inverse cascade. *Phys. Rev. E* 75, 046301.
- SEGALINI, A., ÖRLÜ, R., SCHLATTER, P., ALFREDSSON, H. P., RÜEDI, J.-D. & TALAMELLI, A. 2011 A method to estimate turbulence intensity and transverse

- Taylor microscale in turbulent flows from spatially averaged hot-wire data. Exp. Fluids 51, 693–700.
- SHINGAI, K. & KAWAMURA, H. 2002 Direct numerical simulation of turbulent heat transfer in the stably stratified Ekman layer. *Therm. Sci. Eng.* **10**, 25.
- SHINGAI, K. & KAWAMURA, H. 2004 A study of turbulence structure and large-scale motion in the Ekman layer through direct numerical simulations. J. Turb. 5 (1).
- SILLERO, J. A., JIMÉNEZ, J. & MOSER, R. D. 2013 One-point statistics for turbulent wall-bounded flows at Reynolds numbers up to $\delta^+ \approx 2000$. Phys. Fluids 25, 105102.
- SKAMAROCK, W. C. 2004 Evaluating mesoscale NWP models using kinetic energy spectra. *Mon. Weather Rev.* **132** (12), 3019–3032.
- SMAGORINSKY, J. 1963 General circulation experiments with the primitive equations.

 Mon. Weather Rev. 91, 99.
- SMITH, L. M. & Waleffe, F. 1999 Transfer of energy to two-dimensional large scales in forced, rotating three-dimensional turbulence. *Phys. Fluids* **11**, 1608.
- SPALART, P. R. 1988 Direct simulation of a turbulent boundary layer up to $Re_{\theta} = 1410$. J. Fluid Mech. 187, 61–98.
- Spalart, P. R. 1989 Theoretical and numerical study of a three-dimensional turbulent boundary layer. *J. Fluid Mech.* **205**, 319–340.
- Spalart, P. R., Coleman, G. N. & Johnstone, R. 2008 Direct numerical simulation of the Ekman layer: A step in Reynolds number, and cautious support for a log law with a shifted origin. *Phys. Fluids* **20**, 101507.
- Spalart, P. R., Coleman, G. N. & Johnstone, R. 2009 Retraction: "Direct numerical simulation of the Ekman layer: A step in Reynolds number, and cautious support for a log law with a shifted origin". *Phys. Fluids* **21** (10), 109901.
- SREENIVASAN, B. & DAVIDSON, P. A. 2008 On the formation of cyclones and anticyclones in a rotating fluid. *Phys. Fluids* **20**, 085104.
- STAPLEHURST, P. J., DAVIDSON, P. A. & DALZIEL, S. B. 2008 Structure formation in homogeneous freely decaying rotating turbulence. *J. Fluid Mech.* **598** (1), 81–105.
- Stolz, S. & Adams, N. A. 1999 An approximate deconvolution procedure for large-eddy simulation. *Phys. Fluids* **11** (7), 1699–1701.
- Takahashi, Y. O., Hamilton, K. & Ohfuchi, W. 2006 Explicit global simulation of the mesoscale spectrum of atmospheric motions. *Geophys. Res. Lett.* **33**, L12812.
- Tatro, P. R. & Mollo-Christensen, E. L. 1966 Experiments on Ekman layer instability. PhD thesis, Cambridge Univ Press.
- Taylor, G. I. 1923 Experiments on the motion of solid bodies in rotating fluids. *Proc. R. Soc. Lond.*, A **104**, 213–218.
- Taylor, J. R. & Sarkar, S. 2007 Internal gravity waves generated by a turbulent bottom Ekman layer. J. Fluid Mech. 590, 331–354.
- Taylor, J. R. & Sarkar, S. 2008a Direct and large eddy simulations of a bottom Ekman layer under an external stratification. *Int. J. of Heat and Fluid Flow* **29** (3), 721–732.
- Taylor, J. R. & Sarkar, S. 2008b Stratification effects in a bottom Ekman layer. J. Phys. Oceanogr. 38 (11), 2535–2555.
- Thompson, R. 2005 Explanation of spc severe weather parameters.

- TOWNSEND, A. A. 1976 The Structure of Turbulent Shear Flow. Cambridge University Press.
- TSINOBER, A. & LEVICH, E. 1983 On the helical nature of three-dimensional coherent structures in turbulent flows. *Phys. Lett. A* **99** (6), 321–324.
- VALLGREN, A. 2011 Infrared Reynolds number dependency of the two-dimensional inverse energy cascade. J. Fluid Mech. 667, 463–473.
- Vallgren, A., Deusebio, E. & Lindborg, E. 2011 A possible explanation of the atmospheric kinetic and potential energy spectra. *Phys. Rev. Lett.* **99**, 99–101.
- VALLGREN, A. & LINDBORG, E. 2011 The enstrophy cascade in forced twodimensional turbulence. J. Fluid Mech. 671, 168–183.
- Vallis, G. K. 2006 Atmospheric and Oceanic Fluid Dynamics: Fundamentals and Large-scale Circulation; electronic version. Leiden: Cambridge Univ. Press.
- WAITE, M. L. & BARTELLO, P. 2006 The transition from geostrophic to stratified turbulence. J. Fluid Mech. 568, 89–108.
- Waite, M. L. & Snyder, C. 2009 The mesoscale kinetic energy spectrum of a baroclinic life cycle. J. Atmos. Sci. 66, 883.
- Waleffe, F. 1993 Inertial transfers in the helical decomposition. Phys. Fluids 5, 677.
- DE WIEL, B. J. H. V., MOENE, A. F. & JONKER, H. J. J. 2012 The cessation of continuous turbulence as precursor of the very stable nocturnal boundary layer. J. Atmos. Sci. 69 (11), 3097–3115.
- Wyngaard, J. C. 1973 On surface-layer turbulence. Workshop in Micrometeorology pp. 101–149, Boston.
- XIA, H., BYRNE, D., FALKOVICH, G. & SHATS, M. 2011 Upscale energy transfer in thick turbulent fluid layers. *Nat. Phys.* **7** (4), 321–324.
- ZHEMIN, T. & RONGSHENG, W. 1994 Helicity dynamics of atmospheric flow. Adv. Atmos. Sci. 11 (2), 175–188.
- ZILITINKEVICH, S. S., ELPERIN, T., KLEEORIN, N., ROGACHEVSKII, I., ESAU, I., MAURITSEN, T. & MILES, M. W. 2008 Turbulence energetics in stably stratified geophysical flows: Strong and weak mixing regimes. *Quart. J. Roy. Meteor. Soc.* 134 (633), 793–799.
- ZILITINKEVICH, S. S. & ESAU, I. 2007 Similarity theory and calculation of turbulent fluxes at the surface for the stably stratified atmospheric boundary layer. *Boun.-Lay. Meteorol.* **125** (2), 193–205.